Transcriptional assessment by microarray analysis and large scale meta-analysis of the metabolic capacity of cardiac and skeletal muscle tissues to cope with reduced nutrient availability in gilthead sea bream (*Sparus aurata* L.)

Josep A. Calduch-Giner[1], Yann Echasseriau[2], Diego Crespo[3], Daniel Baron[4], Josep V. Planas[3], Patrick Prunet[2] & Jaume Pérez-Sánchez[1]

[1]Nutrigenomics and Fish Growth Endocrinology Group, Instituto de Acuicultura Torre de la Sal (IATS-CSIC), Castellón, Spain

[2]INRA, UR1037 LPGP Fish Physiology and Genomics, Rennes, France

[3]Departament de Fisiologia i Immunologia, Facultat de Biologia, Universitat de Barcelona and Institut de Biomedicina de la Universitat de Barcelona (IBUB), Barcelona, Spain

[4]INSERM, UMR 1064, Nantes, France

Running title: cardiac and skeletal muscle transcriptome

Corresponding author: Jaume Pérez-Sánchez

e-mail: jaime.perez.sanchez@csic.es

Tel: +34 964319500

Fax: +34 964319509

Abstract

The effects of nutrient availability on the transcriptome of cardiac and skeletal muscle tissues was assessed in juvenile gilthead sea bream fed with a standard diet at two feeding levels: i) full ration size and ii) 70% satiation followed by a finishing phase at the maintenance ration. Microarray analysis evidenced a characteristic transcriptomic profile for each muscle tissue following changes in oxidative capacity (heart > red skeletal muscle > white skeletal muscle). The transcriptome of heart and secondly that of red skeletal muscle were highly responsive to nutritional changes, whereas that of glycolytic white skeletal muscle showed less ability to respond. The highly expressed and nutritionally regulated genes of heart were mainly related to signal transduction and transcriptional regulation. In contrast, those of white muscle were enriched in gene ontology (GO) terms related to proteolysis and protein ubiquitination. Microarray meta-analysis using the bioinformatic tool Fish and Chips (http://fishandchips.genouest.org/index.php) showed the close association of a representative cluster of white skeletal muscle with some of cardiac and red skeletal muscle, and many GO terms related to mitochondrial function appeared to be common links between them. A second round of cluster comparisons revealed that mitochondria-related GOs also linked differentially expressed genes of heart with those of liver from cortisol-treated gilthead sea bream. These results show that mitochondria are among the first responders to environmental and nutritional stress stimuli in gilthead sea bream, and functional phenotyping of this cellular organelle is highly promising to obtain reliable markers of growth performance and well-being in this fish species.

Key words: feeding level, skeletal muscle, heart, microarray, meta-analysis, mitochondria.

Background

The optimization and modelling of muscle fish growth is an intended goal of the aquaculture industry to improve its productivity, sustainability and profitability. Indeed, large quantities of fish larvae are produced, but survival rates are often low or highly variable, and in most cases the growth potential of cultured fish is not fully exploited (Conceição et al., 2010). This is indicative of important gaps in our knowledge, and understanding the mechanisms by which the environment, and nutrient availability and diet composition in particular, introduce growth variability among individuals and fish species is an important goal for future aquaculture research (Valente et al., 2013). In this sense, it must be noted that myogenesis is a common feature of all vertebrates, and the relative timing and importance of production (hyperplasia) and subsequent enlargement (hypertrophy) of muscle fibers determines the growth potential and the final weight attained by a given species (Johnston, 2006; Johnston et al., 2011).

As key components of muscle growth, the first genes to be targeted are the myogenic regulatory factors myoD, myf5, myogenin and MRF4 (Fernandes et al., 2007; Hinits et al., 2009; Rescan, 2001), and those related with the insulin and somatotropic axes (Glass, 2005; Oksbjerg et al., 2004). Hence, considered as a whole, the components of the somatotropic axis (growth hormone, GH; insulin-like growth factors, IGFs; IGF-binding proteins; IGF-receptors; GH receptors) are highly informative of the metabolic condition and growth potential arising from the changing environment and nutritional condition year-round and through the productive cycle in either salmonid (Gómez-Requeni et al., 2005) or non-salmonid fish (Benedito-Palos et al., 2007; Mingarro et al., 2002; Pérez-Sánchez et al., 2002; Saera-Vila et al., 2007; Saera-Vila et al., 2009). With the advent of new genomic tools (Baron et al., 2007b), it is expected that new genes and processes, regulated by environmental factors, controlling key traits

to maximize muscle growth will be recognized and characterized. For instance, the use of fish-specific microarrays has allowed the simultaneous expression of thousands of transcripts to be compared in a number of experiments, and have proven to be a valuable tool in many genomic studies in the field of aquaculture (Prunet et al., 2012). In particular for gilthead sea bream (*Sparus aurata* L.), many specific microarrays have been employed to analyze the transcriptionally-mediated changes on ontogeny (Ferraresso et al., 2008), skin and scales regeneration (Vieira et al., 2011), cortisol administration (Sarropoulou et al., 2005; Teles et al., 2013), crowding stress (Calduch-Giner et al., 2010), and parasite and nutritional challenges (Davey et al., 2011; Calduch-Giner et al., 2012). However, experimental designs are focused on a few specific research questions, that lead to a rather limited set of conditions and replicates, and integration of results for a broad range of species and experimental conditions are still far to be achieved. Besides, available Atlas of gene expression clearly indicate that the expression profile in mammals, and perhaps other vertebrates, is quite different among organs and tissues (Briggs et al., 2011; Son et al., 2005).

To solve the above issues, integrative approaches of functional genomics have enormous potential for the association of a given phenotype and process to a particular gene expression profile (Feichtinger et al., 2012; Moreau et al., 2003). Taking this into account, the aim of this work was to assess by microarray analysis the functional regulation in gilthead sea bream of the transcriptome of cardiac and skeletal muscle (white and red) tissues in a model of restricted nutrient availability. This analysis was completed by the search of common gene signatures and biological processes in the muscle tissues exposed to food restriction in the present experiment and other transcriptomic studies carried out in fish. For that analysis, we used a newly developed bioinformatic tool (Fish and Chips, http://fishandchips.genouest.org).

Materials and methods

Experimental setup and sampling

Juvenile gilthead sea bream were acclimatized to laboratory conditions for 25 days before the start of the trial in the indoor experimental facilities of the Institute of Aquaculture Institute Torre de la Sal (IATS-CSIC). After this initial period, fish of 17.08±0.06 g initial mean body mass were randomly distributed into 500 L-tanks in triplicate groups of 50 fish each. Fish were fed from May to August (11 weeks) with a commercial diet (D-2 Excel 1P, Skretting, Stavanger, Norway) twice per day at two different feeding levels: i) full ration until visual satiety (R_{100}) and ii) 70% satiation for 8 weeks followed by a finishing phase at the maintenance ration for 3 weeks ($R_{70\text{-}20}$). The trial was conducted under natural photoperiod and temperature conditions at IATS latitude (40°5N; 0°10E, 16-25 ºC). Water flow was 20 L/min, oxygen content of water effluents was always higher than 85% saturation, and unionized ammonia remained below toxic levels (< 0.02 mg/L).

At the end of the trial (following an overnight fasting), eight fish per dietary treatment (three from two of the triplicate tanks and two from the third one) were anesthetized with 100 mg/L of 3-aminobenzoic acid ethyl ester (MS-222, Sigma-Aldrich, Madrid, Spain). Heart ventricles and tissue samples of white and red skeletal muscles were rapidly excised, frozen in liquid nitrogen and stored at -80°C until RNA extraction. All procedures were carried out according to the national (IATS-CSIC Review Board) and the current EU legislation on the handling of experimental animals.

RNA Extraction

Total RNA from target tissues was isolated with the ABI PRISM™ 6100 Nucleic Acid PrepStation (Applied Biosystems, Foster City, CA, USA). Briefly, tissue samples were homogenized at a ratio of 25 mg/mL with a guanidine–detergent lysis reagent. The reaction mixture was treated with proteinase K, and RNA purification was achieved by passing the tissue lysate (0.4–0.5 mL) through a purification tray containing an application-specific membrane. Wash solutions containing DNase were applied, and total RNA was eluted into a 96-well PCR plate. The RNA yield was 30–50 μg with absorbance measures (A260/280) of 1.9–2.1, and RIN (RNA integrity number) measurements using the Agilent 2100 Bioanalyzer varied between 8 and 10, which is indicative of clean and intact RNA suitable for microarray analysis.

Microarray hybridizations

Sequences present on the gilthead sea bream oligonucleotide microarray were obtained from the EST collection of the Spanish Consortium Aquagenomics. This array was designed with the eArray online tool (Agilent Technologies, Santa Clara, CA, USA), and contained 2-3 different 60-mer probes for each of the 6862 transcripts encoding for annotated sequences (20,499 total different probes), as well as a unique probe for each of the 8294 sequences with no annotation. The design of the array is stored in the NCBI Gene Expression Omnibus (GEO) database under accession GPL13442. RNA labelling, hybridizations and scanning were performed according to the manufacturer's instructions. Briefly, total RNA (100 ng) from each individual sample was amplified and Cy3-labelled with Agilent One-Color Microarray-Based Gene Expression analysis (Low Input Quick Amp Labelling kit) along with Agilent One-color RNA SpikeIn kit. After labelling, cRNA was purified with RNeasy mini spin columns (Qiagen, Chatsworth, CA, USA) and quantity and quality was checked using a

nanodrop (Thermo Scientific, Wilgminton, DE, USA) and 2100 Bioanalyzer (Agilent), respectively. Each RNA sample (1.65 µg) was then hybridized to the gilthead sea bream array at 65ºC for 17 h using the Agilent GE hybridization kit. After washing, arrays were scanned with the Agilent scanner G2505B. Spot intensities and other quality control features were extracted using the Agilent Feature Extraction software version 10.4.0.0, and were deposited in GEO under accession identifier GSE47859.

Microarray data analysis

Microarray data were analyzed by means of the GeneSpring GX 11.5.1 software (Agilent) focusing on the probes encoding annotated sequences. The quality of each individual hybridization was assessed with the Feature Extraction plug-in (Agilent). To verify that all features within each array were measured over the same starting intensity, raw data (median intensity of each spot) were extracted and corrected for background with the same plug-in. To remove systematic signal intensity bias between each array, data were log2 transformed and normalized as previously described (Kuroka et al., 2013) using the "75th percentile shift", the recommended global normalization method by Agilent for alignment of intensities distributions across arrays for comparisons (see Agilent Technologies, 2009). To ensure similar expression of all transcripts, a baseline transformation was applied by subtracting for each probe the median value of its intensities (Baron et al., 2005). The quality and comparability of samples before and after normalization was verified by analysis of intensity boxplots and MA plots.

Further statistical analyses included a principal components analysis of the six experimental groups, as well as an one-way ANOVA (corrected P-value < 0.05, Tukey's HSD post hoc test, Benjamini-Hochberg multiple testing correction) and k-means clustering of the differentially expressed genes. Gene ontology (GO) and Fisher

enrichment analyses of k-means clusters were carried out by means of Blast2GO software (Conesa et al., 2005).

Real-time qPCR validation

Up to 11 genes representative of all k-means clusters of differentially expressed genes were validated by real-time qPCR on the same individual RNA samples used for cDNA labelling for microarray analysis, using a MyiQ Real-Time PCR Detection System (Bio-Rad, Hercules, CA, USA). Synthesis of cDNA was performed with the High-Capacity cDNA Archive Kit (Applied Biosystems, Foster City, CA, USA) using random decamers. For this purpose, 500 ng of total RNA was reverse-transcribed in a final volume of 100 µl. RT reactions were incubated for 10 min at 25ºC followed by 2 h at 37ºC. Negative control reactions were incubated in the absence of reverse transcriptase. PCR reactions (20 µl of final volume) contained 10 µl of SYBR GreenER qPCR SuperMix (Invitrogen, Gaithersburg, MD, USA), 500 nM of forward and reverse specific primers (Table 1), and 5 µl of diluted cDNA. Reactions were run using the following protocol: 2 min at 50°C, 8 min at 95°C, followed by 40 cycles of 15 s denaturation at 95°C and 30 s at 60°C, and a final melting curve of 81 cycles from 55 to 95°C (0.5°C increments every 10 s). β-Actin was used as the housekeeping gene and the efficiency of PCR reactions for target and reference genes was always higher than 90%. The dynamic range of standard curves (serial dilutions of RT-PCR reactions) spanned five orders of magnitude, and the amount of product in a particular sample was determined by interpolation of the cycle threshold (Ct) value. The specificity of the reaction was verified by analysis of melting curves. Fluorescence data acquired during the extension phase were ultimately normalized to β-actin by the ΔΔCt method (Livak and Schmittgen, 2001). Results are expressed as mean fold-change ± standard error of

the mean (SEM) with respect to the control group, which was set at 1 (Table 2). Statistical differences ($P < 0.05$) were calculated by non parametric Mann-Whitney U-test for the determination of differences among groups, using StatView 5.0 (SAS Institute, Cary, NC, USA). The expression of β-actin was not affected by feeding level in any tissue.

Microarray meta-analysis

Identification of co-regulated transcript groups among tissues was performed with the Fish and Chips online tool (http://fishandchips.genouest.org). This resource, specifically designed for the meta-analysis of fish-related microarray experiments, has been constructed in a similar way to the MADmuscle database (Baron et al., 2011b). The database was thus built by the reanalysis of datasets from public (GEO and ArrayExpress) and private repositories, and populated with clusters of co-expressed genes generated from these datasets. The corresponding gene lists were used as the basis for pair-wise comparisons with the user's list.

Public datasets were pre-processed and normalized using a channel-by-channel Lowess procedure (Workman et al., 2002) adapted to the analysis of mono- (Baron et al., 2007a; Baron et al., 2011a) and two-channel (Lamirault et al., 2010; Quillé et al., 2011) microarrays. After this normalization step, clusters were identified by a stable k-means procedure, applied on log and baseline transformed data (Baron et al., 2007a). The quality of each cluster was then evaluated by a test statistic based on the Pearson's product-moment coefficient. For standardization, gene annotation was performed mapping transcript sequences retrieved from NCBI on Ensembl annotated genomes using a BLAST strategy. For each sequence, the best match (Ensembl Gene ID) on a fish genome was retained. Orthology/paralogy relationships between annotated genes

were computed from Ensembl BioMart tool and gathered in the database as previously described (Baron et al., 2011b). Besides, functional annotation of the clusters (gene lists) was performed using the GOMiner program (Zeeberg et al., 2003) and the Gene Ontology resource (Ashburner et al., 2000).

In order to identify similar trends of co-expression across datasets from the database, the search tool performs a statistical comparison of the input gene list from the user and the lists from the database related to the clusters. The concordance of similarity (overlap) between lists was indicated by the ratio between the number of common genes (size of the overlapping list) and the total number of genes (size of the input list). Its statistical relevance was evaluated by the Fisher's exact test. Besides, among the results, the ability of the targeted output cluster to statistically discriminate between experimental conditions (stress vs. control) was evaluated by the Fisher's exact test as previously described (Feuerstein et al., 2012).

Currently, the database contains the datasets from 355 microarray experiments from public and private repositories (listed in Supplemental Table A1) up to April 2013, which were conducted on zebrafish (*Danio rerio*, H.) (188 datasets), European sea bass (*Dicentrarchus labrax*, L.) (4 datasets), Atlantic cod (*Gadus morhua*, L.) (5 datasets), longjaw mudsucker (*Gillichthys mirabilis,* C.*)* (4 datasets), rainbow trout (*Oncorhynchus mykiss*, W.) (73 datasets), Atlantic salmon (*Salmo salar*, L.) (60 datasets) and gilthead sea bream (21 datasets). All datasets were included together in an automatic lowess re-normalization and re-analysis to identify clusters of co-expressed genes that are functionally annotated. Statistically significant GO annotations in gene clusters were determined by Fisher's exact test.

Results

Fish growth performance

Fish of the R_{100} group grew from 17.06±0.07 to 72.55±0.20 g (SGR = 1.95±0.01), with a feed efficiency (wet weight gain/dry feed intake) of 0.89±0.04. In the $R_{70\text{-}20}$ group the final body weight (48.67±0.13 g, SGR = 1.41±0.01) and feed efficiency (0.11±0.01) were significantly lower. For more detail see Bermejo-Nogales et al. (2011).

Tissue-specific transcriptome profile

Principal component analysis of microarray results clearly grouped together the transcriptomes of the same tissue regardless of dietary treatment (Figure 1). Component 1 contributed to most of the variation (69.9%), and separated the different muscle tissues according to their oxidative capacity (white skeletal muscle < red skeletal muscle < heart). These inter-tissue differences were also evidenced when dietary samples of each tissue were grouped and analyzed by means of one-way ANOVA, finding a differential expression for 3499 genes. The k-means clustering of these differentially expressed genes established three major groups of genes, reflecting the different transcript abundance among muscle tissues. The WM-cluster was composed of 1393 annotated genes that were expressed at a higher level (more than 4-fold on average) in the white skeletal muscle than in the red skeletal muscle or heart (Figure 2A). A second cluster with 628 annotated genes was termed the RM-cluster, as the red skeletal muscle was the muscle tissue where they reached their greatest expression level (Figure 2B). Likewise, the Heart cluster comprised 1478 annotated genes that were highly expressed in heart in comparison with the other two muscle tissues (Figure 2C).

The tissue-specific transcript expression profile was also regulated by feed restriction, but the magnitude of change did not necessarily reflect the abundance of

transcripts in a given tissue. Hence, genes of the WM-cluster were mostly up- or down-regulated by feed restriction in heart (518 genes; 226 up-regulated and 292 down-regulated) or red skeletal muscle (448 genes; 371 up-regulated and 77 down-regulated) than in the white skeletal muscle, where only 175 genes were differentially expressed by feed restriction (78 genes up-regulated and 97 down-regulated) (Figure 2A). The same transcript expression pattern was found for the other two gene clusters, which was especially evident for the Heart-cluster, with only 3 genes differentially expressed in the white skeletal muscle instead of 242 in the red skeletal muscle or 362 in the heart (Figures 2B and 2C).

Differentially expressed genes by feed restriction were functionally examined by GO analysis. In the white skeletal muscle, the 175 differentially expressed genes of the WM-cluster showed a significant enrichment in processes related to the GO terms "proteolysis", "ubiquitin-dependent catabolic process" and "protein ubiquitination" (Figure 3A). The 90 genes of the RM-cluster that were nutritionally regulated by feed restriction in the red skeletal muscle did not evidence enrichment in any GO process (Figure 3B). Ontologies for the 362 heart-like genes differentially regulated by feed restriction in heart were enriched in the GO terms "signal transduction", "regulation of transcription" and "signalling pathway" (Figure 3C). For each of the analyzed groups, the entire list of differentially expressed genes accompanied by their values of fold-change with feed restriction is presented in Supplemental Tables A2-A4.

Real-time qPCR validation

Three or four genes representative of each tissue-gene cluster (11 in total) were chosen to validate microarray results by qPCR, covering a wide range of up- and down-regulation with restricted feeding. As shown in Table 2, qPCR values were quite

consistent with those of the microarray analysis for 10 of the 11 genes assayed (r=0.91). The only exception to this good correlation was the measured expression of pyruvate dehydrogenase isoenzyme 2 in heart, with a large up-regulation (23.6) with restricted feeding calculated by microarray analysis and a lower fold-change increase (2.24) estimated by means of qPCR validation. Importantly, the expression of all genes analyzed was significantly regulated in response to restricted feeding, except in the case of novel protein similar to vertebrate myelin expression factor 2 in heart (1.48 fold-change).

Microarray meta-analysis

The normalization and clustering steps of the datasets stored in the bioinformatic tool Fish and Chips do not take into account the experimental conditions of each experiment, so a first step in the cluster comparison analysis was the choice of a group of genes with a sample clustering distribution in accordance with the dietary treatment. For the whole set of transcriptome data of white skeletal muscle, the Fish and Chips tool identified 23 clusters that varied in size from 23 to 861 probes, and cluster 17 was selected as the starting point of the meta-analysis because it showed good, and perhaps the best distribution of the samples according to the experimental feed restriction (R_{100} and $R_{70\text{-}20}$). This cluster was composed of 533 probes that corresponded to 224 different annotated genes, and k-means clustering clearly separated the two experimental conditions. Among the five most representative GO terms in cluster 17 of white muscle, the tool revealed the involvement of proteolysis and ubiquitin-protein ligase activity, similar to that which was previously observed by microarray analysis. Profile comparison of this cluster among the fish datasets of Fish and Chips evidenced that the best hits (p-value<0.0001) with cluster 17 of the white skeletal muscle were clusters of

red skeletal muscle and heart derived from the same experimental setup (Figure 4A). Interestingly, many GO terms related to mitochondria function appeared to be common links among the best hit clusters. A second round of cluster comparison with the cluster found in heart (cluster 17, composed by 501 annotated genes) evidenced a significant overlap of genes from clusters from two early developmental stages of gilthead sea bream (from Ferraresso et al., 2008) and from liver transcripts of gilthead sea bream with high plasma cortisol levels induced by slow-release cortisol implants (Teles et al., 2013). The top GO terms of the gilthead sea bream larvae cluster were related to spindle assembly checkpoint and organelle fission, but mitochondria GO terms were again among the major cluster nexus in the cortisol administration experiment (Figure 4B). Overlapping annotated genes between clusters in the first and second round of cluster comparison are listed in Supplemental Table A5.

Discussion

Multiple microarray studies in different animal models, including monkey, rodents, pig, and *Drosophila melanogaster*, have addressed the effect of caloric restriction or food deprivation on transcript expression (Dejean et al., 2007; Gershman et al., 2007; Higami et al., 2004; Kayo et al., 2001; Lkhagvadorj et al., 2010; Martin et al., 2009; Sreekumar et al., 2002; Teleman et al., 2008; Zinke et al., 2002). Even though the duration and the degree of caloric restriction varied among separate studies, common responses are observed, and adipose tissues show a strong down-regulation of energy-generating processes (Higami et al., 2004; Lkhagvadorj et al., 2010; Teleman et al., 2008). Also, the liver shows a strong up-regulation of genes involved in gluconeogenesis (pyruvate metabolism) and β-oxidation, whereas genes linked to oxidative phosphorylation and tricarboxylic acid cycle are down-regulated (Bauer et al.,

2004; Dejean et al., 2007; Desert et al., 2008; Teleman et al., 2008). The muscle tissues show a much weaker response, although caloric restriction in humans leads to enhanced mitochondrial activity (Civitarese et al., 2007). In the same way, feed restriction in gilthead sea bream increases the activity of key metabolic enzymes (citrate synthase, 3-hydroxyacyl CoA dehydrogenase, pyruvate kinase, lactate dehydrogenase) of white skeletal muscle, whereas the mRNA expression of muscle markers of mitochondrial respiration uncoupling (uncoupling protein 3, UCP3) remains mostly unaltered (Bermejo-Nogales et al. 2011). In contrast, in the same study, we also found that UCP3 mRNA expression is highly regulated by feeding level in heart and red skeletal muscle, which is viewed as part of the different tissue muscle strategies to cope with the altered metabolic needs and risk of oxidative stress upon feed restriction or starvation. Our present results complement and expand this hypothesis, although the focus of the study is not pointed on specific genes, but on ontogenies and metabolic pathways derived from the simultaneous differential expression of many transcripts.

The notion of a tissue-specific transcript expression pattern for cardiac and skeletal muscle tissues was further evidenced herein with the simultaneous expression analysis of more than 6000 annotated genes. Hence, the PCA analysis highlighted that the tissue variable is a more discriminant factor that dietary intervention, which allowed a reduction in weight gain of more than 40%. The different transcript expression profile of red and white muscle fibres has also been evidenced by deep RNA-seq in rainbow trout, which showed a predominance of genes involved in protein degradation by means of the ubiquitin-proteasome pathway in the white skeletal muscle (Palstra et al., 2013). Likewise, the tissue-specific transcriptome of human and rodents is usually clustered based on tissue function and developmental origin (Son et al., 2005; Zheng-Bradley et al., 2010). As a result, up to 90% of genes in the human gene expression Atlas are

differentially expressed among the different organs and tissues (Lukk et al., 2010). Thus, the search of general biomarkers of fish performance and growth becomes more complicated, as the establishment of reference expression values for potential candidate genes will be highly dependent on the tissues to be analyzed.

The strength of the molecular tools of analysis is envisaged to greatly increase soon for gilthead sea bream, not only by the growing technical capacity to detect and quantify more transcripts, but also by the improvement of their annotation. Hence, an important number of transcripts from whole larvae (Yúfera et al., 2012), vertebrae and gill arches (Vieira et al., 2013) and skeletal muscle (Garcia de la Serrana et al., 2012) have been recently released, and the conventional Sanger sequencing of several EST libraries combined with next generation sequencing of 454 libraries of intestine, head kidney, blood and skeletal muscle allowed the annotation of more than 75% of the codifying gilthead sea bream transcriptome (Calduch-Giner et al., 2013) in a fully searchable database (http://nutrigroup-iats.org/seabreamdb). In any case, the current version of the presented microarray was designed and annotated prior to some of these recent advances, so the annotation level of the included sequences was around 45%. Regardless of this, one of the strongest effects of nutrient availability on the transcriptome of the white skeletal muscle was reported for stearoyl-CoA desaturases (SCD) with Δ-9 desaturase activity, which have evolved through evolution of the teleost lineage as duplicated genes (Castro et al., 2011). This has been recently confirmed in gilthead sea bream by phylogenetic and sequence analyses of two fatty acid desaturase enzymes of SCD1-type (Benedito-Palos et al., 2013). In particular, the down-regulation of SCD transcripts was especially evident for the SCD1a isoform. This metabolic feature, which was confirmed by qPCR, is not surprising given that SCD enzymes are strong markers of lipogenesis in humans and rodents with a low SCD expression and

activity in obesity and insulin resistance (Hulver et al., 2005; Ntambi et al., 2002; Sampath & Ntambi, 2011).

Protein synthesis and degradation are part of healthy muscle growth and metabolism, and the ubiquitin-proteasome pathway plays a pivotal role in the degradation of short-lived proteins that are important in a variety of basic cellular processes (Jung et al., 2009; Lecker et al., 2006). Prior to degradation, a target protein undergoes a three-step process that covalently links a polyubiquitin chain to the substrate. Three enzyme components are involved in this process (E1-3), and herein the non-specific Ub-conjugating enzymes (E2) were highly represented within the differentially expressed genes of the white muscle of restricted fed fish. Up to six E2 enzymes are consistently down-regulated and the loss of protein deposition with reduced growth would be related to a coordinated decrease of protein synthesis and degradation, as pointed out in different fish models (Fraser & Rogers, 2007). Feed deprivation also modulates other proteases in our experimental model, and the expression of the muscle-specific calpain 3 was significantly down-regulated (fold-change, -2.08) with the concomitant up-regulation (fold-change, 2.05) of the calpain-specific inhibitor (calpastatin). Likewise, Cleveland et al. (2009) have reported a coordinated and opposite regulation of the calpain-calpastatin system in the white muscle of fasted rainbow trout. In any case, at least in our model of nutrient availability, the nutritionally-mediated effects on the transcriptome of white muscle are less evident that those observed in aerobic muscle tissues (heart and red skeletal muscle). One might speculate that this differential regulation at the transcriptional level represents a lower capacity of the glycolytic white muscle to cope with different nutritional and environmental challenges.

Regarding cardiac muscle, many activators of transcription (like chromodomain helicase DNA binding protein 4, dynamin-2, friend leukemia integration 1 transcription factor, GC-rich sequence DNA-binding factor candidate isoform 1, or lysine-specific demethylase 5B and 5B-like, among others) were up-regulated by restricted feeding, whereas transcription inhibitors (notably chibby homolog 1, chromobox protein homolog 5 or origin recognition complex subunit 2) were mostly down-regulated, which conform and extent an overall enhanced transcription. This is specially supported by the up-regulation of dynamin-2, already known as a survival factor for bovine endothelial cells (Kang-Decker et al., 2007). Conversely, the transcription activator ets variant gene 5, involved in cell growth and differentiation, was down-regulated, but even so the augmented expression of this gene is associated with several mouse cardiomyopathies (Spurney et al., 2008). Intriguingly, four-and-a-half LIM domains protein 2 is a well characterized marker of muscle hyperplasia in gilthead sea bream (Rafael et al., 2012), and its down-regulation in the present study might reflect a reduced growth-promoting capability of muscle cardiac tissue. In the same line, we also reported a down-regulation of chibby protein that inhibits cardiomyocyte differentiation of murine embryonic stem cells (Singh et al., 2007). Taken together, these results suggest the activation of mechanisms focused not only in tissue differentiation or growth, but also in tissue cell survival.

Likewise, the up-regulation of a high number of transcripts related to cell signalling GO terms (signal transduction, signalling pathway) (Supplemental Table 4) might be indicative of an adaptive response to keep the life-essential functions of heart. Noteworthy, the consistent up-regulated expression of the pyruvate dehydrogenase kinase isoenzyme 2 is in accordance with the the observed increase of pyruvate dehydrogenase kinase activity in the skeletal muscle of starved rats, driving a reduced

glucose oxidation (Fuller & Randle, 1984; Sugden et al., 2000). Otherwise, the growth factor receptor-bound protein 14 belongs to a family of adaptor molecules involved in insulin receptor signalling (Holt & Siddle, 2005), and its up-regulated expression in our restricted feeding model agrees with a healthy heart phenotype in mice (Lin et al., 2010). Finally, the signal transducer and activator of transcription 3 (STAT3) is required for cardiomyocyte protection (reviewed in Haghikia et al., 2011). So, in our study, the up-regulation of the STAT3 inhibitor (PIAS3) is apparently a contradictory result, but PIAS protein family are not restricted to the inhibition of STATs, and other potential beneficial effects might be considered as reviewed by Schmidt & Müller (2003). As a whole, a highly coordinated action of transcription and cell signalling pathways would serve to maintain heart as an efficient and reliable pump even in face of an adverse metabolic condition, driving the switches of metabolic fuels according the nutrient availabilities (Taegtmeyer et al., 2004). The up-regulated expression of the myogenic growth factor MYOD2 fish could be indicative of this issue in our experimental model of severe feed restriction.

Transcriptomic meta-analysis approaches constitute an alternative to alleviate the methodological constraints due to different tissue responsiveness, comparing data across independent studies to reveal robust biomarkers and pathways for traits of interest. A major pitfall of such meta-analysis is the use of different microarray protocols and platforms, which difficults the comparison among transcriptome datasets (Baron et al., 2011). To date, meta-analytic studies applied to cultured fish performance have been conducted by the revision and classification of published studies for evaluation of the effect of the replacement of live feed on the mortality and growth of freshwater fish larvae at first feeding (47 studies) (Sales, 2011), or the levels of inclusion and source of plant proteins in feed on the growth of salmonids (19 and 45

studies, respectively) (Hua and Bureau, 2012; Collins et al., 2013). Thus, the present work, using the Fish and Chips bioinformatic tool, represents the first time that a meta-analysis based on genomic data from a vast repository with many different experimental setups, species and microarray types has been conducted in a fish species of aquaculture interest. Semi-automatization of normalization and clustering has allowed the inclusion of a significant number of datasets, 355 to date, that cover a wide array of experimental conditions, species and tissues. The annotation by means of GO terms also facilitates the determination of common pathways in multi-tissue comparisons. Taking these issues into account, two rounds of gene cluster comparisons served to highlight the key role of mitochondria, not only in the transcriptomic response in both aerobic and anaerobic muscle tissues in response to feed restriction, but also to link the mitochondria in the stress response mediated by cortisol administration. This notion is also supported by previous gilthead sea bream studies in which different mitochondrial-related genes, including antioxidant enzymes, respiratory chain components, and mitochondrial chaperones and heat shock proteins, have been identified as highly stress-responsive genes in crowding stress models combined with a different nutritional background as the result of the use of either fish oil or a blend of alternative vegetable oils as the most important dietary lipid source (Calduch-Giner et al., 2010; Pérez-Sánchez et al., 2013). This is, in fact, not surprising given that the mitochondrion is an important cellular organelle housing the oxidative phosphorylation machinery and multiple metabolic pathways such as β-oxidation of fatty acids and the tricarboxylic acid and urea cycles. In addition, mitochondria have important biosynthetic activities, control intracellular calcium metabolism and signalling, generate most cellular reactive oxygen species (ROS) and serve as the gatekeeper of the cell for apoptosis, facing a vast array of disturbance setups in different tissues, as reviewed by Liesa et al. (2009).

In summary, cardiac and skeletal muscle tissues of gilthead sea bream evidenced a clear distinctive transcript expression pattern. Nutritionally regulated genes with a high level of expression in the glycolytic white muscle were mostly related to proteolysis and protein ubiquitination pathways, whereas aerobic muscles shared an extensive response, which might reflect the metabolic plasticity of muscle tissues with essential physiological functions. The microarray meta-analysis highlighted the tissue-specific differences of the fish transcriptome among tissues, fish species and experimental conditions, but also evidenced the emerging role of mitochondria as a common link, despite the different oxidative capacities of cardiac and skeletal muscle tissues. This opens new research possibilities focusing on mitochondria as a reliable subcellular marker of stress phenotyping in fish and gilthead sea bream in particular.

Acknowledgments

This work was funded by the EU seventh Framework Programme by the AQUAEXCEL (Aquaculture Infrastructures for Excellence in European Fish Research, FP7/2007-2012; grant agreement nº 262336) project. Additional funding was obtained from the Generalitat Valenciana (research grant PROMETEO 2010/006) and the Spanish Government through AQUAGENOMICS project (Consolider-Ingenio-2010 Programme).

References

Ashburner M, Ball CA, Blake JA, Botstein D, Butler H, Cherry JM, Davis AP, Dolinski K, Dwight SS, Eppig JT, Harris MA, Hill DP, Issel-Tarver L, Kasarskis A, Lewis S, Matese JC, Richardson JE, Ringwald M, Rubin GM, Sherlock G (2000) Gene ontology: tool for the unification of biology. The Gene Ontology Consortium. Nat Genet 25:25-29

Agilent Technologies (2009) One-color microarray-based gene expression analysis (Quick Amp Labeling) with Tecan HS Pro Hybridization. Publication number G4140-90041. Available: http://www.chem.agilent.com/library/usermanuals/public/g4140-90041_one-color_tecan.pdf

Baron D, Bihouée A, Teusan R, Dubois E, Savagner F, Steenman M, Houlgatte R, Ramstein G (2011a) MADGene: retrieval and processing of gene identifier lists for the analysis of heterogeneous microarray datasets. Bioinformatics 27(5):725-726

Baron D, Dubois E, Bihouée A, Teusan R, Steenman M, Jourdon P, Magot A, Peréon Y, Veitia R, Savagner F, Ramstein G, Houlgatte R (2011b) Meta-analysis of muscle transcriptome data using the MADMuscle database reveals biologically relevant gene patterns. BMC Genomics 12:113

Baron D, Houlgatte R, Fostier A, Guiguen Y (2005) Large-scale temporal gene expression profiling during gonadal differentiation and early gametogenesis in rainbow trout. Biol Reprod 73:959-966

Baron D, Magot A, Ramstein G, Steenman M, Fayet G, Chevalier C, Jourdon P, Houlgatte R, Savagner F, Pereon Y (2011c) Immune response and mitochondrial metabolism are commonly deregulated in DMD and aging skeletal muscle. PLoS One 6:e26952

Baron D, Montfort J, Houlgatte R, Fostier A, Guiguen Y (2007a) Androgen-induced masculinization in rainbow trout results in a marked dysregulation of early gonadal gene expression profiles. BMC Genomics 8:357

Baron D, Raharijaona M, Houlgatte R (2007b) DNA microarrays. IRBM 28:210-215

Bauer M, Hamm AC, Bonaus M, Jacob A, Jaekel J, Schorle H, Pankratz MJ, Katzenberger JD (2004) Starvation response in mouse liver shows strong correlation with life-span-prolonging processes. Physiol Genomics 17:230-244

Beckman BR (2011) Perspectives on concordant and discordant relations between insulin-like growth factor (IGF1) and growth in fishes. Gen Comp Endocrinol 170:233-252

Benedito-Palos L, Calduch-Giner JA, Ballester-Lozano GF, Pérez-Sánchez J (2013) Effect of ration size on fillet fatty acid composition, phospholipid allostasis and mRNA

expression patterns of lipid regulatory genes in gilthead sea bream (*Sparus aurata*). British J Nutr 109:1175-1187

Benedito-Palos L, Saera-Vila A, Calduch-Giner JA, Kaushik S, Pérez-Sánchez J (2007) Combined replacement of fish meal and oil in practical diets for fast growing juveniles of gilthead sea bream (*Sparus aurata* L.): Networking of systemic and local components of GH/IGF axis. Aquaculture 267:199-212

Bermejo-Nogales A, Benedito-Palos L, Calduch-Giner JA, Pérez-Sánchez J (2011) Feed restriction up-regulates uncoupling protein 3 (UCP3) gene expression in heart and red muscle tissues of gilthead sea bream (*Sparus aurata* L.). New insights in substrate oxidation and energy expenditure. Comp Biochem Physiol A. 159:296-302

Brand MD, Affourtit CA, Esteves TC, Green K, Lambert AJ, Miwa S, Pakay JL, Parker N (2004) Mitochondrial superoxide: production, biological effects, and activation of uncoupling proteins. Free Radical Biol Med 37:755-767

Briggs J, Paoloni M, Chen QR, Wen X, Khan J, Khanna C (2011) A compendium of canine normal tissue gene expression. PLoS One 6:e17107

Calduch-Giner JA, Bermejo-Nogales A, Benedito-Palos L, Estensoro I, Ballester-Lozano G, Sitjà-Bobadilla A, Pérez-Sánchez J (2013) Deep sequencing for *de novo* construction of a marine fish (*Sparus aurata*) transcriptome database with a large coverage of protein-coding transcripts. BMC Genomics 14:178

Calduch-Giner JA, Davey G, Saera-Vila A, Houeix B, Talbot A, Prunet P, Cairns MT, Pérez-Sánchez J (2010) Use of microarray technology to assess the time course of liver stress response after confinement exposure in gilthead sea bream (*Sparus aurata* L.). BMC Genomics 11:193

Calduch-Giner JA, Sitjà-Bobadilla A, Davey GC, Cairns MT, Kaushik S, Pérez-Sánchez J (2012) Dietary vegetable oils do not alter the intestine transcriptome of gilthead sea bream (*Sparus aurata*), but modulate the transcriptomic response to infection with *Enteromyxum leei*. BMC Genomics 13:470

Castro LFC, Wilson JM, Gonçalves O, Galante-Oliveira S, Rocha E, Cunha I (2011) The evolutionary history of the stearoyl-CoA desaturase gene family in vertebrates. BMC Evol Biol 11:132

Civitarese AE, Carling S, Heilbronn LK, Hulver MH, Ukropcova B, Deutsch WA, Smith SR, Ravussin E (2007) Calorie restriction increases muscle mitochondrial biogenesis in healthy humans. PLoS Med 4:e76

Cleveland BM, Weber GM, Blemings KP, Silverstein JT (2009) Insulin-like growth factor-I and genetic effects on indexes of protein degradation in response to feed deprivation in rainbow trout (*Oncorhynchus mykiss*). Am J Physiol Regul Integr Comp Physiol 297:R1332-1342

Collins SA, Øverland M, Skrede A, Drew MD (2013) Effect of plant protein sources on growth rate in salmonids: Meta-analysis of dietary inclusion of soybean, pea and canola/rapeseed meals and protein concentrates. Aquaculture 400-401:85-100

Conceição, L.E.C., Aragão, Richard N, Engrola S, Gavaia P, Mira S, Dias J (2010) Novel methodologies in marine fish larval nutrition. Fish Physiol Biochem 36:1-16

Conesa A, Götz S, García-Gómez JM, Perol J, Talón M, Robles M (2005) Blast2GO: a universal tool for annotation, visualization and analysis in functional genomics research. Bioinformatics 21:3674-3676

Davey GC, Calduch-Giner JA, Houeix B, Talbot A, Sitjà-Bobadilla A, Prunet, P, Pérez-Sánchez J, Cairns MT (2011) Molecular profiling of the gilthead sea bream (*Sparus aurata* L.) response to chronic exposure to the myxosporean parasite *Enteromyxum leei*. Molecular Immunology 48:2102-2112

Dejean S, Martin PG, Baccini A, Besse P (2007) Clustering time-series gene expression data using smoothing spline derivatives. EURASIP J Bioinform Syst Biol 70561

Desert C, Duclos MJ, Blavy P, Lecerf F, Moreews F, Klopp C, Aubry M, Herault F, Le Roy P, Berri C, Douaire M, Diot C, Lagarrigue S (2008) Transcriptome profiling of the feeding-to-fasting transition in chicken liver. BMC Genomics 9:611

Feichtinger J, McFarlane RJ, Larcombe LD (2012) CancerMA: a web-based tool for automatic meta-analysis of public cancer microarray data. Database bas055

Fernandes JMO, Kinghorn JR, Johnston IA (2007) Differential expression of multiple alternatively spliced transcripts of MyoD. Gene 391:178-185

Ferraresso S, Vitulo N, Mininni AN, Romualdi C, Cardazzo B, Negrisolo E, Reinhardt R, Canario AVM, Patarnello T Bargelloni L (2008) Development and validation of a gene expression oligo microarray for the gilthead sea bream (*Sparus aurata*). BMC Genomics 9:580

Feuerstein P, Puard V, Chevalier C, Teusan R, Cadoret V, Guerif F, Houlgatte R, Royere D (2012) Genomic assessment of human cumulus cell marker genes as predictors of oocyte developmental competence: impact of various experimental factors. PLoS One 7:e40449

Fuller SJ, Randel PJ (1984) Reversible phosphorylation of pyruvate dehydrogenase in rat skeletal-muscle mitochondria. Effects of starvation and diabetes. Biochem J 219:635-646

Garcia de la Serrana D, Estévez A, Andree K, Johnston IA (2012) Fast skeletal muscle transcriptome of the gilthead sea bream (*Sparus aurata*) determined by next generation sequencing. BMC Genomics 13:181

Gershman B, Puig O, Hang L, Peitzsch RM, Tatar M, Garofalo RS (2007) High resolution dynamics of the transcriptional response to nutrition in Drosophila: a key role for dFOXO. Physiol Genomics 29:24-34

Glass DJ (2005) Skeletal muscle hypertrophy and atrophy signalling pathways. Int J Bioch Cell Biol 37:1974-1984

Gómez-Requeni P, Calduch-Giner J, Vega-Rubín de Celis S, Medale F, Kaushik S, Pérez-Sánchez J (2005) Regulation of somatotropic axis by dietary factors in rainbow trout (*Onchorhynchus mykiss*). British Journal of Nutrition 94:353-361

Higami Y, Pugh TD, Page GP, Allison DB, Prolla TA, Weindruch R (2004) Adipose tissue energy metabolism: altered gene expression profile of mice subjected to long-term caloric restriction. FASEB J 18:415-417

Hinits Y, Osborn DP, Hughes SM (2009) Differential requirements for myogenic regulatory factors distinguish medial and lateral somitic, cranial and fin muscle fibre populations. Development 136:403-14

Holt LJ, Siddle K (2005) Grb10 and Grb14: enigmatic regulators of insulin action – and more?. Biochem J 388:393–406

Hua K, Bureau DP (2012) Exploring the possibility of quantifying the effects of plant protein ingredients in fish feeds using meta-analysis and nutritional model simulation-based approaches. Aquaculture 356-357:284-301

Hulver MW, Berggren JR, Carper MJ, Miyazaki M, Ntambi JM, Hoffman EP, Thyfault JP, Stevens R, Dohm GL, Houmard JA, Muoio DM (2005) Elevated stearoyl-CoA desaturase-1 expression in skeletal muscle contributes to abnormal fatty acid partitioning in obese humans. Cell Metab 2:251-261

Johnston I (2006) Environment and plasticity of myogenesis in teleost fish. J Exp Biol 209:2249-2264

Johnston IA, Bower NI, Macqueen DJ (2011) Growth and the regulation of myotomal muscle mass in teleost fish. J Exp Biol 214:1617-16228

Johnston IA, Manthri S, Bickerdike R, Dingwall A, Luijkx R, Campbell P, Nickell D, Alderson R (2004) Growth performance, muscle structure and flesh quality in out-of-season Atlantic salmon (*Salmo salar*) smolts reared under two different photoperiod regimes. Aquaculture 237:281-300

Jung T, Catalgol B, Grune T (2009) The proteasomal system. Mol Aspects Med 30:191-296

Kang-Decker N, Cao S, Chatterjee S, Yao J, Egan LJ, Semela D, Mukhopadhyay D, Shah V (2007) Nitric oxide promotes endothelial cell survival signaling through S-nitrosylation and activation of dynamin-2. J Cell Sci 120:492-501

Kayo T, Allison DB, Weindruch R, Prolla TA (2001) Influences of aging and caloric restriction on the transcriptional profile of skeletal muscle from rhesus monkeys. Proc Natl Acad Sci USA 98:5093-5098

Kurokawa K, Akaike Y, Masuda K, Kuwano Y, Nishida K, Yamagishi N, Kajita K, Tanahashi T, Rokutan K (2013) Downregulation of serine/arginine-rich splicing factor 3 induces G1 cell cycle arrest and apoptosis in colon cancer cells. Oncogene 2013 doi: 10.1038/onc.2013.86

Lamirault G, Meur NL, Roussel JC, Cunff MF, Baron D, Bihouée A, Guisle I, Raharijaona M, Ramstein G, Teusan R, Chevalier C, Gueffet JP, Trochu JN, Léger JJ, Houlgatte R, Steenman M (2010) Molecular risk stratification in advanced heart failure patients J Cell Mol Med 14:1443-1452

Lecker SH, Goldberg AL, Mitch WE (2006) Protein Degradation by the Ubiquitin–Proteasome Pathway in Normal and Disease States. J Am Soc Nephrol 17:1807-1819

Liesa M, Palacín M, Zorzano A (2009) Mitochondrial dynamics in mammalian health and disease. Physiol Rev 89:799-845

Lin RCY, Weeks KL, Gao X-M, Williams RBH, Bernardo BC, Kiriazis H, Matthews VB, Woodcock EA, Bouwman RD, Mollica JP, Speirs HJ, Dawes IW, Daly RJ, Shioi T, Izumo S, Febbraio MA, Du X-J, McMullen JR (2010) PI3K(p110α) Protects Against Myocardial Infarction-Induced Heart Failure: Identification of PI3K-Regulated miRNA and mRNA. Arterioscler Thromb Vasc Biol 30:724-732

Livak KJ, Schmittgen TD (2001) Analysis of relative gene expression data using real-time quantitative PCR and the $2^{-\Delta\Delta C}{}_T$ method. Methods 25:402-408

Lkhagvadorj S, Qu L, Cai W, Couture OP, Barb CR, Hausman GJ, Nettleton D, Anderson LL, Dekkers JC, Tuggle CK (2010) Gene expression profiling of the short-term adaptive response to acute caloric restriction in liver and adipose tissues of pigs differing in feed efficiency. Am J Physiol Regul Integr Comp Physiol 298:R494-R507

Lukk M, Kapushesky M, Nikkilä J, Parkinson H, Goncalves A, Huber W, Ukkonen E, Brazma A (2010) A global map of human gene expression. Nat Biotechnol 28:322-324

Martin B, Pearson M, Brenneman R, Golden E, Wood W, Prabhu V, Becker KG, Mattson MP, Maudsley S (2009) Gonadal transcriptome alterations in response to dietary energy intake: sensing the reproductive environment. PLoS ONE 4:e4146

Mingarro M, Vega-Rubín de Celis S, Astola A, Pendón C, Valdivia MM, Pérez-Sánchez J (2002) Endocrine mediators of seasonal growth in gilthead sea bream: The growth hormone and somatolactin paradigm. Gen Comp Endocrinol 128:102-111

Mommsen TP (2001) Paradigms of growth in fish. Comp Biochem Physiol B. 129:207-219

Moreau Y, Aerts S, De MB, Dabrowski M (2003) Comparison and meta-analysis of microarray data: from the bench to the computer desk. Trends Genet 19:570-577

Nabben M, Hoeks J (2008) Mitochondrial uncoupling protein 3 and its role in cardiac- and skeletal muscle metabolism. Physiol Behav 94:259-269

Ntambi JM, Miyazaki M, Stoehr JP, Lan H, Kendziorski CM, Yandell BS, Song Y, Cohen P, Friedman JM, Attie AD (2002) Loss of stearoyl-CoA desaturase-1 function protects mice against adiposity. Proc Natl Acad Sci USA 99:11482-11486

Oksbjerg N, Gondret F, Vestergaard M (2004) Basic principles of muscle development and growth in meat-producing mammals as affected by the insulin-like growth factor (IGF) system. Domest Anim Endocrinol 27:219-240

Palstra AP, Beltran S, Burgerhout E, Brittijn SA, Magnoni LJ, Henkel CV, Jansen HJ, van den Thillart GEEJM, Spaink SP, Planas JV (2013) Deep RNA sequencing of the skeletal muscle transcriptome in swimming fish. PLoS ONE 8:e53171

Pérez-Sánchez J, Borrel M, Bermejo-Nogales A, Benedito-Palos L, Saera-Vila A, Calduch-Giner JA, Kaushik S (2013) Dietary oils mediate cortisol kinetics and the hepatic mRNA expression profile of stress-responsive genes in gilthead sea bream (*Sparus aurata*) exposed to crowding stress. Implications on energy homeostasis and stress susceptibility. Comp Biochem Physiology D 8:123-130

Pérez-Sánchez J, Calduch-Giner J, Mingarro M, Vega-Rubín de Celis S, Gómez-Requeni P, Saera-Vila A, Astola A, Valdivia MM (2002) Overview of fish growth hormone family. New insights in genomic organization and heterogeneity of fish growth hormone receptors. Fish Physiol Biochem 27:243-258

Prunet P, Øverli Ø, Douxfils J, Bernardini G, Kestemont P, Baron D (2012) Fish Welfare and genomics. Fish Physiol Biochem 38:43-60

Quillé ML, Carat S, Quéméner-Redon S, Hirchaud E, Baron D, Benech C, Guihot J, Placet M, Mignen O, Férec C, Houlgatte R, Friocourt G (2011) High-throughput analysis of promoter occupancy reveals new targets for Arx, a gene mutated in mental retardation and interneuronopathies. PLoS One 6:e25181

Rafael MS, Laizé V, Bensimon-Brito A, Leite RB, Schüle R, Cancela ML (2012) Four-and-a-half LIM domains protein 2 (FHL2) is associated with the development of craniofacial musculature in the teleost fish *Sparus aurata*. Cell Mol Life Sci 69:423-434

Rescan PY (2001) Regulation and functions of myogenic regulatory factors in lower vertebrates. Comp Biochem Physiol B 130:1-12

Saera-Vila A, JA Calduch-Giner, Pérez-Sánchez J (2007) Co-expression of IGFs and GH receptors (GHRs) in gilthead sea bream (*Sparus aurata* L.): sequence analysis of the GHR-flanking region. J Endocrinol 194:361-372

Saera-Vila A, Calduch-Giner JA, Prunet P, Pérez-Sánchez J (2009) Dynamics of liver GH/IGF axis and selected stress markers in juvenile gilthead sea bream (*Sparus aurata*) exposed to acute confinement. Differential stress response of growth hormone receptors. Comp Biochem Physiol A 154:197-203

Sales J (2011) First feeding of freshwater fish larvae with live feed versus compound diets: a meta-analysis. Aquacult Int 19:1217-1228

Sampath H, Ntambi JM (2011) The role of stearoyl-CoA desaturase in obesity, insulin resistance, and inflammation. Ann NY Acad Sci 1243:47-53

Sarropoulou E, Kotoulas G, Power DM, Geisler R (2005) Gene expression profiling of gilthead sea bream during early development and detection of stress-related genes by the application of cDNA microarray technology. Physiological Genomics 23:182-191

Schmidt D, Müller S (2003) PIAS/SUMO: new partners in transcriptional regulation. Cell Mol Life Sci 60:2561-2574

Singh AM, Li F-Q, Hamazaki T, Kasahara H, Takemaru K-H, Terada N (2007) Chibby, an antagonist of the Wnt/β-catenin Pathway, facilitates cardiomyocyte differentiation of murine embryonic stem cells. Circulation 115:617–626

Son CG, Bilke S, Davis S, Greer BT, Wei JS, Whiteford CC, Chen Q-R, Cenacchi N, Khan J (2005) Database of mRNA gene expression profiles of multiple human organs. Genome Res 15:443-50

Spurney CF, Knoblach S, Pistilli EE, Nagaraju K, Martin GR, Hoffman EP (2008) Dystrophin-deficient cardiomyopathy in mouse: Expression of Nox4 and Lox are associated with fibrosis and altered functional parameters in the heart. Neuromuscular Disorders 18:371–381

Sreekumar R, Unnikrishnan J, Fu A, Nygren J, Short KR, Schimke J, Barazzoni R, Nair KS (2002) Effects of caloric restriction on mitochondrial function and gene transcripts in rat muscle. Am J Physiol Endocrinol Metab 283:E38-E43

Sugden MC, Kraus A, Harris RA, Holness MJ (2000) Fibre-type specific modification of the activity and regulation of skeletal muscle pyruvate dehydrogenase kinase (PDK) by prolonged starvation and refeeding is associated with targeted regulation of PDK isoenzyme 4 expression. Biochem J 346:651-657

Taegtmeyer H, Golfman L, Sharma S, Razeghi P, van Arsdall M (2004) Linking gene expression to function: metabolic flexibility in the normal and diseased heart. Ann N Y Acad Sci:202–213

Teleman AA, Hietakangas V, Sayadian AC, Cohen SM (2008) Nutritional control of protein biosynthetic capacity by insulin via Myc in Drosophila. Cell Metab 7:21-32

Teles M, Boltaña S, Reyes-López F, Santos MA, Mackenzie S, Tort L (2013) Effects of chronic cortisol administration of GR and the liver transcriptome in *Sparus aurata*. Mar Biotechnol 15:104-114

Valente LMP, Moutou KA, Conceição LEC, Engrola S, Fernandes JMO, Johnston IA (2013) What determines growth potential and juvenile quality of farmed fish species?. Reviews in Aquaculture 5:S168-S193

Vieira FA, Gregório SF, Ferraresso S, Thorne MAS, Costa R, Milan M, Bargelloni L, Clark MS, Canario AVM, Power DM (2011) Skin healing and scale regeneration in fed and unfed sea bream *Sparus auratus*. BMC Genomics 12:490

Vieira FA, Thorne MAS, Stueber K, Darias M, Reinhardt R, Clark MS, Gisbert E, Power DM (2013) Comparative analysis of a teleost skeleton transcriptome provides insight into its regulation. Gen Comp Endocrinol 191:45-58

Workman C, Jensen LJ, Jarmer H, Berka R, Gautier L, Nielser HB, Saxild HH, Nielsen C, Brunak S, Knudsen S (2002) A new non-linear normalization method for reducing variability in DNA microarray experiments. Genome Biol 3:research0048

Yúfera M, Halm S, Beltrán S, Fusté B, Planas JV, Martínez-Rodríguez G (2012) Transcriptomic characterization of the larval stage in gilthead sea bream (*Sparus aurata*) by 454 pyrosequencing. Mar Biotechnol 14:423-435

Zeeberg BR, Feng W, Wang G, Wang MD, Fojo AT, Sunshine M, Narasimhan S, Kane DW, Reinhold WC, Lababidi S, Bussey KJ, Riss J, Barrett JC, Weinstein JN (2003) GoMiner: a resource for biological interpretation of genomic and proteomic data. Genome Biol 4:R28

Zheng-Bradley X, Rung J, Parkinson H, Brazma A (2010) Large scale comparison of global gene expression patterns in human and mouse. Genome Biol 11:R124

Zinke I, Schutz CS, Katzenberger JD, Bauer M, Pankratz MJ (2002) Nutrient control of gene expression in Drosophila: microarray analysis of starvation and sugar dependent response. EMBO J 21:6162-6173

Table 1. Primers used for real-time qPCR.

GenBank/Probe Name	Description	Primer sequence (5´-3´)	Amplicon size (bp)
CUST_16662_PI419285025	Makorin-1	(F) ACGAGGACGAAGAGATGGTGACG (R) GAGTGTTAGTTGGTGGGGCTGCT	170
CUST_7901_PI419285025	Serpin h1 precursor	(F) CCGTGTCTCTGCCCAAAGTCA (R) TCCGTCAGTGTCCCATTCCAT	182
CUST_6095_PI419285025	Delta-9-desaturase 1	(F) GCTGTGTGTTTTGCCGTGTGTAA (R) CTCTTGGCACTGCGATGTATTCA	246
AM967776	Skeletal muscle sodium channel alpha subunit-like	(F) TCTGCTCATCCTGGCTTGGTTTT (R) CACCAGCAGCACATCAAACAGG	226
AM975569	Neural cell adhesion molecule isoform 3	(F) GGTGCGTTGGTGATTGAGGAG (R) TTTGAGGGAGAAGAGGACTGAGGA	171
AM979502	Membrane-type matrix metalloproteinase	(F) GCCTGCCTCGTGGTTACTGA (R) CACAAACACTTACCGCTGACACA	98
CUST_15171_PI419285025	Annexin a2a	(F) GTAAGAAATCAGTCGTCAGCGTCC (R) GCAAAAGAAAAAGTCGGATGAGC	107
CUST_13470_PI419285025	Pyruvate dehydrogenase isoenzyme 2	(F) TGTGTGAGTAGGAGTGGACGGAAA (R) TTTCATCGTCGCAGGCTTCA	105
AM957114	Novel protein similar to vertebrate myelin expression factor 2 (MYEF2)	(F) GGTGGAAATAACATCAGGAAGGGA (R) CATTCAGCCGATAGCCGTTCA	223
AM969068	Androgen receptor	(F) TGACCAATGAGCCAATGTAGCA (R) CAAACCGCCCAACTTACTCAAA	217
AM978198	Adiponectin receptor protein 1	(F) GTTCCTTGGCATTTTGATGTGTTG (R) TACATTGTGCGTAGCCCAGGA	233
X89920	Beta actin	(F) TCCTGCGGAATCCATGAGA (R) GACGTCGCACTTCATGATGCT	51

Table 2. Comparison between microarray results and qPCR validation with the indicated tissues and target genes. Data from microarray and qPCR are expressed in fold-change values.

Tissue	Description	Microarray	qPCR
WM	Makorin-1	3.25	1.88
WM	Serpin h1 precursor	-2.38	-2.63
WM	Delta-9-desaturase 1	-6.26	-16.67
RM	Skeletal muscle sodium channel alpha subunit-like	2.22	2.53
RM	Neural cell adhesion molecule isoform 3	1.84	1.74
RM	Membrane-type matrix metalloproteinase	-1.64	-1.75
RM	Annexin a2a	-2.93	-5.26
Heart	Pyruvate dehydrogenase isoenzyme 2	23.60	2.24
Heart	Novel protein similar to vertebrate myelin expression factor 2 (MYEF2)	2.63	1.48
Heart	Androgen receptor	2.21	2.75
Heart	Adiponectin receptor protein 1	-1.76	-2.04

Figure Legends

Figure 1. Principal components analysis of white skeletal muscle, red muscle and heart transcriptome after feed restriction.

Figure 2. K-means cluster analysis of differentially expressed genes in (A) skeletal white muscle, (B) skeletal red muscle, and (C) cardiac muscle. In each cluster, the tissue with the lowest expression was used as a reference (value 1.0) for fold-change calculations. Down-regulated genes with restricted feeding are represented by green bars, whereas red bars represent up-regulated genes.

Figure 3. Distribution of GO term profiles (biological process, multilevel) of differentially expressed genes. (A) WM-like cluster genes differentially expressed in white muscle, (B) RM-like cluster genes differentially expressed in red muscle, (C) Heart-like cluster genes differentially expressed in heart. Significantly enriched GO terms (Fisher's test, p) are highlighted in yellow.

Figure 4. Output of Fish and Chips meta-analysis. (A) First round of cluster meta-analysis, mitochondria-related GO terms are highlighted. (B) Second round of cluster meta-analysis, mitochondria-related GO terms are highlighted.

Figure 1

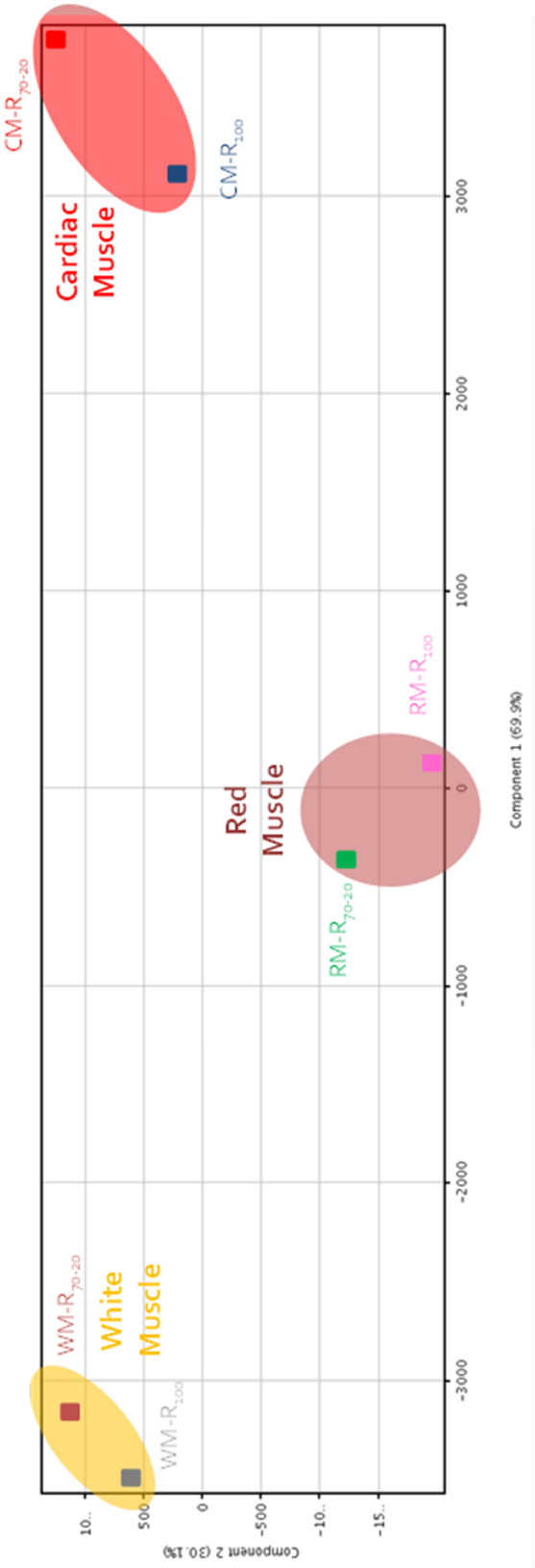
CM-R70-20
CM-R100
Cardiac Muscle
Red Muscle
RM-R100
RM-R70-20
WM-R70-20
White Muscle
WM-R100
Component 1 (69.9%)
Component 2 (30.1%)
3000
2000
1000
0
-1000
-2000
-3000
500
-500
10..
-10..
-15..

Figure 2

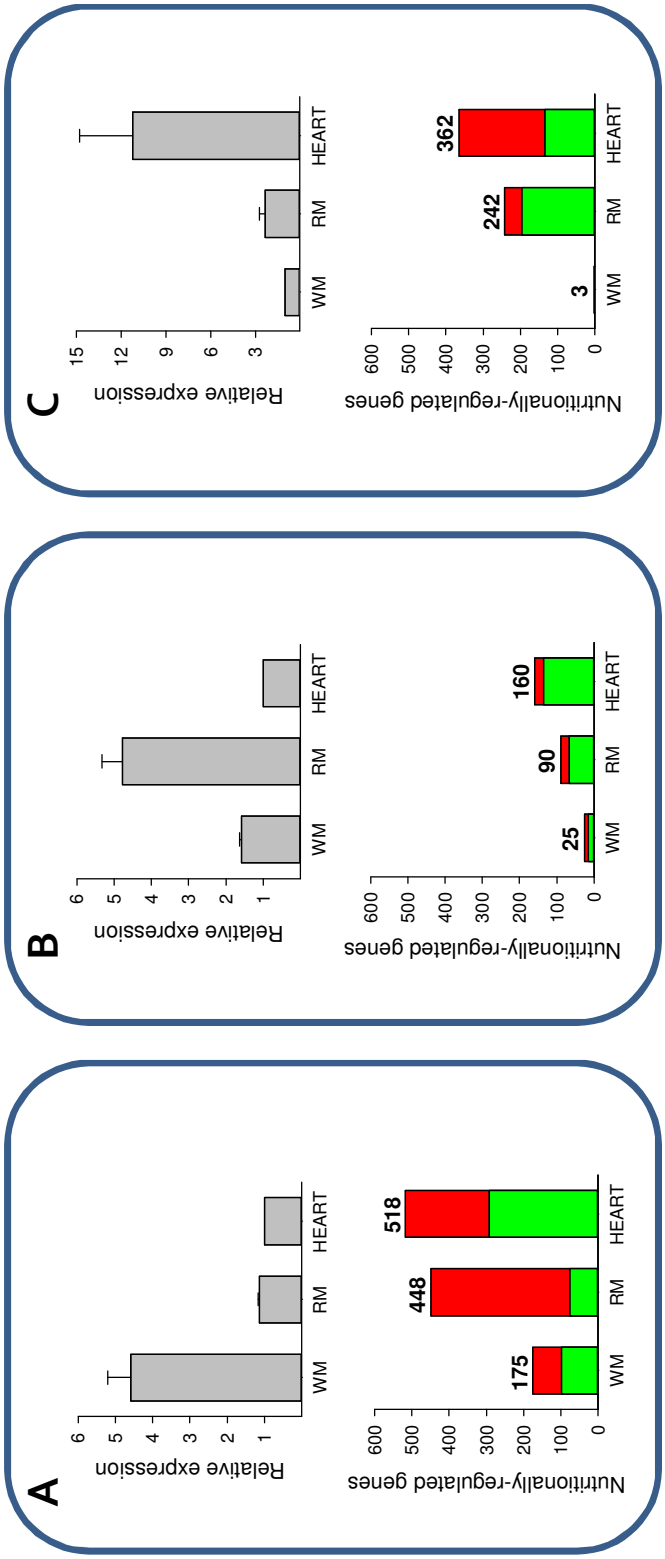
A
Relative expression
Nutritionally-regulated genes
WM
RM
HEART
175
448
518
B
Relative expression
Nutritionally-regulated genes
WM
RM
HEART
25
90
160
C
Relative expression
Nutritionally-regulated genes
WM
RM
HEART
3
242
362

Figure 3

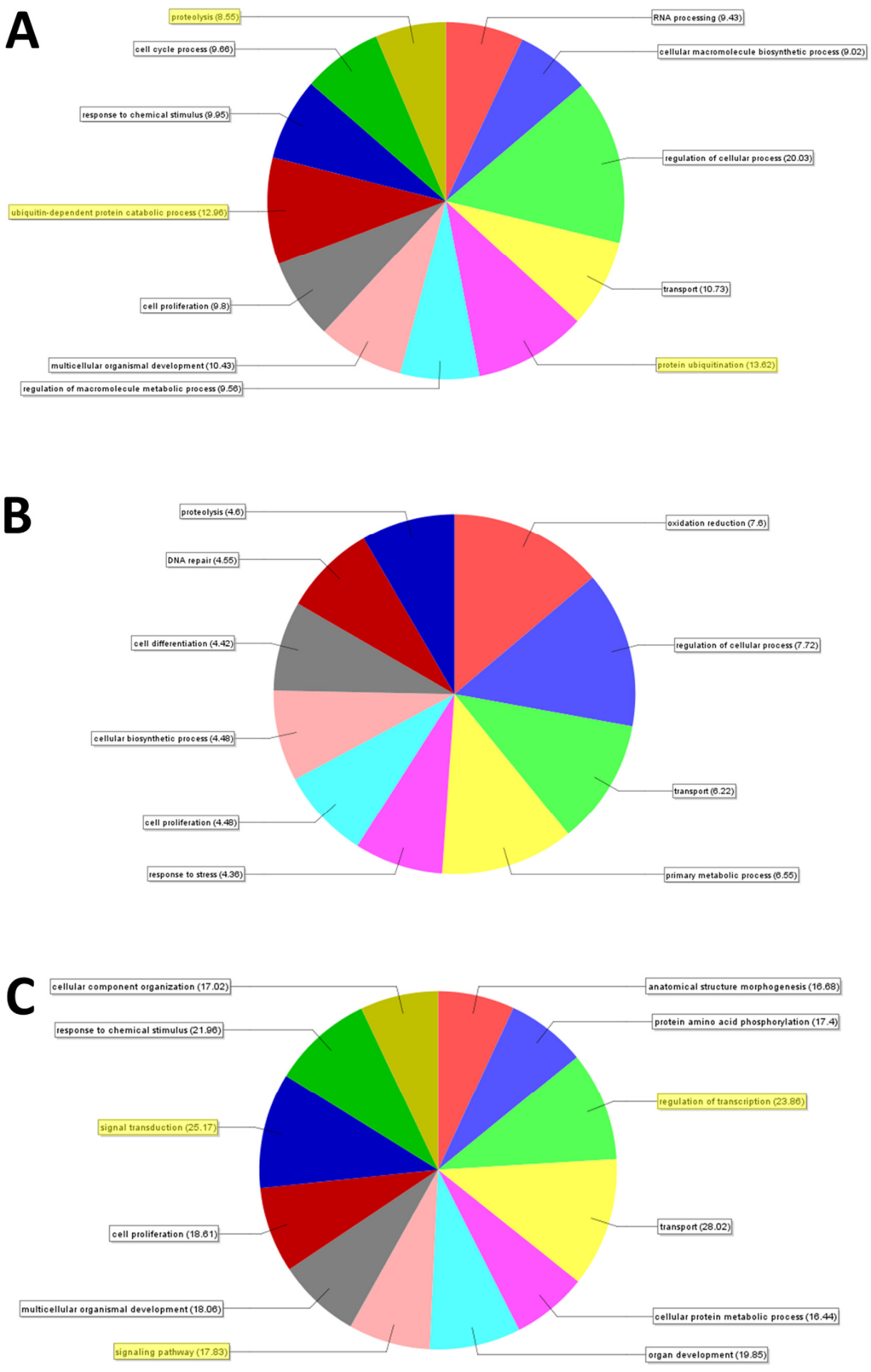
A
proteolysis (8.55)
cell cycle process (9.66)
response to chemical stimulus (9.95)
ubiquitin-dependent protein catabolic process (12.96)
cell proliferation (9.8)
multicellular organismal development (10.43)
regulation of macromolecule metabolic process (9.56)
RNA processing (9.43)
cellular macromolecule biosynthetic process (9.02)
regulation of cellular process (20.03)
transport (10.73)
protein ubiquitination (13.62)
B
proteolysis (4.6)
DNA repair (4.55)
cell differentiation (4.42)
cellular biosynthetic process (4.48)
cell proliferation (4.48)
response to stress (4.36)
oxidation reduction (7.6)
regulation of cellular process (7.72)
transport (6.22)
primary metabolic process (6.55)
C
cellular component organization (17.02)
response to chemical stimulus (21.96)
signal transduction (25.17)
cell proliferation (18.61)
multicellular organismal development (18.06)
signaling pathway (17.83)
anatomical structure morphogenesis (16.68)
protein amino acid phosphorylation (17.4)
regulation of transcription (23.86)
transport (28.02)
cellular protein metabolic process (16.44)
organ development (19.85)

Figure 4

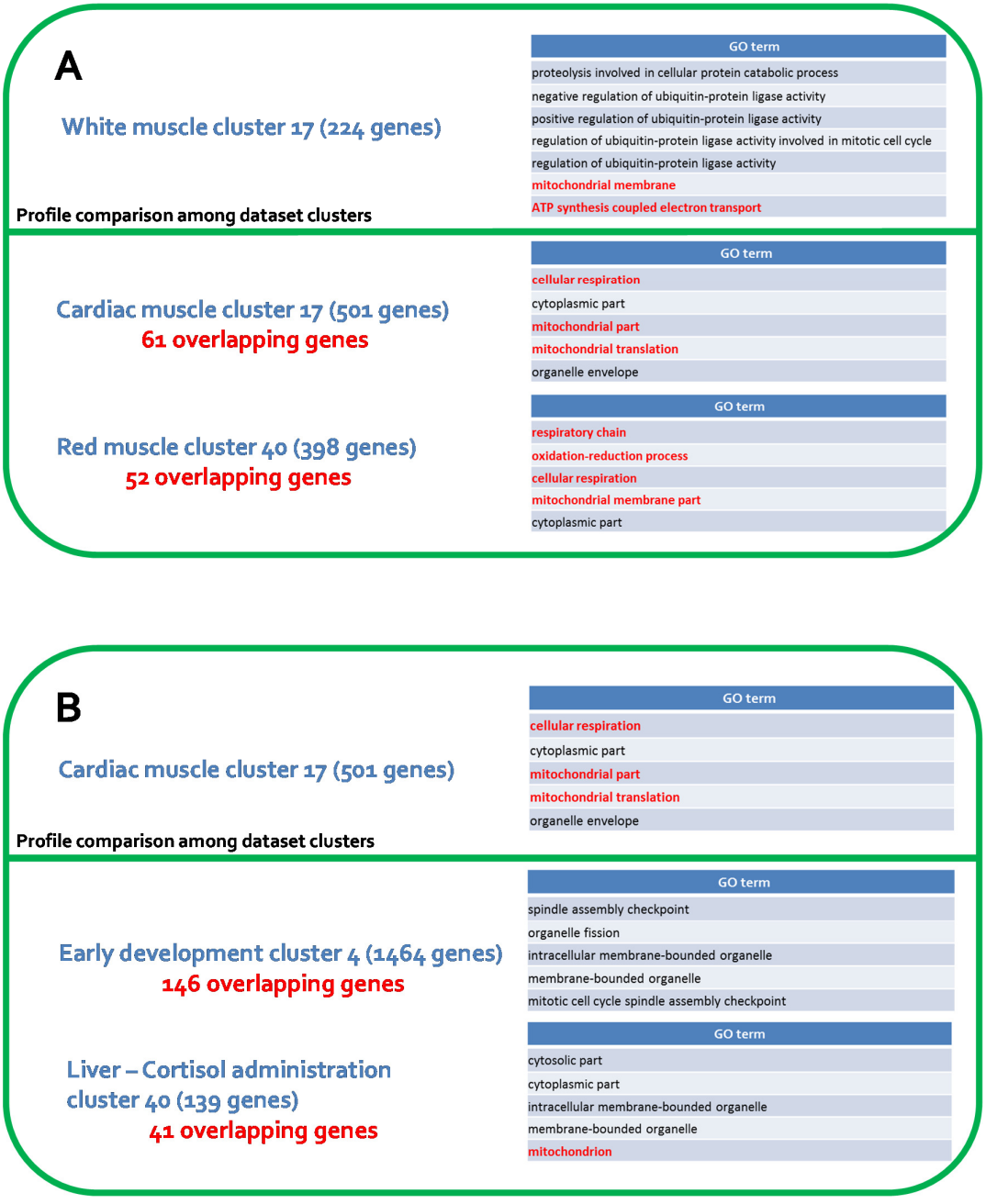
A
White muscle cluster 17 (224 genes)
Profile comparison among dataset clusters
GO term
proteolysis involved in cellular protein catabolic process
negative regulation of ubiquitin-protein ligase activity
positive regulation of ubiquitin-protein ligase activity
regulation of ubiquitin-protein ligase activity involved in mitotic cell cycle
regulation of ubiquitin-protein ligase activity
mitochondrial membrane
ATP synthesis coupled electron transport
Cardiac muscle cluster 17 (501 genes)
61 overlapping genes
GO term
cellular respiration
cytoplasmic part
mitochondrial part
mitochondrial translation
organelle envelope
Red muscle cluster 40 (398 genes)
52 overlapping genes
GO term
respiratory chain
oxidation-reduction process
cellular respiration
mitochondrial membrane part
cytoplasmic part
B
Cardiac muscle cluster 17 (501 genes)
Profile comparison among dataset clusters
GO term
cellular respiration
cytoplasmic part
mitochondrial part
mitochondrial translation
organelle envelope
Early development cluster 4 (1464 genes)
146 overlapping genes
GO term
spindle assembly checkpoint
organelle fission
intracellular membrane-bounded organelle
membrane-bounded organelle
mitotic cell cycle spindle assembly checkpoint
Liver – Cortisol administration cluster 40 (139 genes)
41 overlapping genes
GO term
cytosolic part
cytoplasmic part
intracellular membrane-bounded organelle
membrane-bounded organelle
mitochondrion

Supplementary data

Supplemental table A1. Datasets included in the bioinformatic meta-analysis tool Fish and Chips.

Supplemental table A2. Genes differentially expressed by restricted ration size in white skeletal muscle. Genes sharing the enriched GO terms “protein ubiquitination”, “proteolysis” or “ubiquitin-dependent protein catabolic process” are highlighted in bold.

Supplemental table A3. Genes differentially expressed by restricted ration size in red skeletal muscle.

Supplemental table A4. Genes differentially expressed by restricted ration size in cardiac muscle. Genes sharing the enriched GO terms “regulation of transcription”, “signal transduction” or “signaling pathway” are highlighted in bold.

Supplemental table A5. Overlapping annotated genes between clusters in the first and second round of cluster comparison.

Supplemental table A1.

Dataset accession	Dataset description	Species
GSE3667-GPL1319	1, 3, or 5 Day Post Amputation Vehicle or TCDD Exposed	*Danio rerio*
GSE10766-GPL1319	1Day Post Amputation Vehicle or Beclomethasone Exposed	*Danio rerio*
GSE10184-GPL1319	2 or 3 Day Post Amputation Vehicle or TCDD Exposed	*Danio rerio*
GSE24616-GPL6457	A phylogenetically based transcriptome age index mirrors ontogenetic divergence patterns	*Sparus aurata*
GSE15410-GPL2878	AB* zebrafish embryos exposed to 1 ng/mL TCDD from 1d to 5d post-fertilization.	*Danio rerio*
GSE22462-GPL10169	Acclimation Effects on Acute Thermal Stress in the goby, Gillichthys mirabilis	*Gillichthys mirabilis*
GSE11893-GPL1319	AHR Activation by TCDD Downregulates Sox9b Expression Producing Jaw Malformation in Zebrafish Embryos	*Danio rerio*
GSE10157-GPL2878	Altered gene expression in zebrafish embryos exposed to tert-butylhydroquinone and 2,3,7,8-tetrachlorodibenzo-p-dioxin	*Danio rerio*
GSE17756-GPL9074	An integrated study to the effects of thermal acclimation in zebrafish	*Danio rerio*
GSE19041-GPL9663	Analysis of gene expression profiles on 38 days-old sea bass heads	*Dicentrarchus labrax*
GSE7018-GPL4860	Androgen treatment in female rainbow trout leads to a marked dysregulation of gonadal gene expression profiles	*Oncorhynchus mykiss*
GSE25328-GPL10679	Anti-in?ammatory e?ects of tetradecylthioacetic acid (TTA) in macrophage-like cells from Atlantic salmon (Salmo salar L.)	*Salmo salar*
GSE25328-GPL10705	Anti-in?ammatory e?ects of tetradecylthioacetic acid (TTA) in macrophage-like cells from Atlantic salmon (Salmo salar L.)	*Salmo salar*
E-MTAB-494-A-AFFY-38	Aplexone Targets the HMG-CoA Reductase Pathway and Differentially Regulates Arteriovenous Angiogenesis	*Danio rerio*
GSE18219-GPL8467	Aquafirst_seabream_pathogen exposure_head kidney	*Sparus aurata*
E-TABM-1178-A-MEXP-2053	AQUAMAX cod	*Gadus morhua*
AQUAEXCEL-12	Aquamax foie Dataset	*Oncorhynchus mykiss*
E-TABM-1156-A-MEXP-2058	Atlantic Cod Early Development	*Gadus morhua*
GSE3857-GPL2716	Atlantic Salmon Amoebic Gill Disease Study	*Salmo salar*
GSE1031-GPL966	Atlantic Salmon Head Kidney Study	*Salmo salar*
E-TABM-1213-GPL2716	Atlantic salmon liver transcriptome response to exposure to three human pharmaceuticals	*Salmo salar*
GSE1012-GPL966	Atlantic Salmon Macrophage Study	*Salmo salar*
GSE18830-GPL1319	B1 sox (sox2/3/19a/19b) quadruple knockdown in the zebrafish embryo	*Danio rerio*
GSE9357-GPL4603	biosensor-series	*Danio rerio*
GSE6745-GPL3713	Brain transcriptomics in response to beta-naphthoflavone treatment in rainbow trout: The role of AhR signaling.	*Oncorhynchus mykiss*
GSE17113-GPL7301	Cadmium and temperature probe selection and validation experiment for custom array production	*Danio rerio*
GSE17082-GPL7301	Cadmium probe selection experiment for custom array production	*Danio rerio*
GSE17085-GPL7301	Cadmium validation experiment for custom array production	*Danio rerio*
GSE5091-GPL2899	Cell line stimulated with recombinant cytokines interleukin-1b and interferon gamma.	*Oncorhynchus mykiss*
AQUAEXCEL-13	Chaains foie muscle Dataset	*Oncorhynchus mykiss*
GSE18120-GPL6154	Challenge of vaccinated and unvaccinated salmon with Aeromonas salmonicida	*Salmo salar*
GSE10188-GPL1319	Comparative genomic analysis between adult and larval fin regeneration	*Danio rerio*
GSE9020-GPL1319	Comparative Genomics Identifies Gene Targets for Retinoic Acid in the Embryonic Zebrafish Hearts	*Danio rerio*
E-MTAB-406-A-AFFY-38	Comparative transcription profiling of mouse, chicken and zebrafish in the presomitic mesoderms to identify cyclic genes of the segmentation clock	*Danio rerio*
GSE36860-GPL10705	Comparison of Atlantic salmon individuals with different outcomes of cardiomyopathy syndrome (CMS)	*Salmo salar*
GSE36860-GPL10706	Comparison of Atlantic salmon individuals with different outcomes of cardiomyopathy syndrome (CMS)	*Salmo salar*
GSE21539-GPL1319	Comparison of expression data between control and Ovo1 morphant zebrafish embryos	*Danio rerio*
GSE16721-GPL8731	Comparison of gene expression in the salmon parr precocious and non-precocious testis	*Salmo salar*
GSE19001-GPL9663	Comparison of gene expression profile between 58 days-old prognatous sea bass jaws and control ones	*Dicentrarchus labrax*
GSE18915-GPL6467	Comparison of gene expression profile of gilthead seabream mineralization-induced VSa13 cells against controls	*Sparus aurata*
GSE18941-GPL6467	Comparison of gene expression profile of gilthead seabream mineralization-induced VSa16 cells against controls	*Sparus aurata*
GSE27067-GPL7301	Comparison of genomic, morphological, and behavioral responses among fathead minnow (Pimephales promelas) and zebrafish (Danio rerio) to acute RDX exposure	*Danio rerio*
GSE16860-GPL8704	Comparison of precocious and non-precocious salmon	*Salmo salar*
GSE16860-GPL8731	Comparison of precocious and non-precocious salmon	*Salmo salar*
GSE16720-GPL8704	Comparison of precocious and non-precocious salmon brain	*Salmo salar*
GSE22221-GPL6563	Comparison of retinal gene expression in wild-type and XOPS-mCFP (rod degeneration) transgenic zebrafish	*Danio rerio*
GSE11493-GPL1319	Comparison of transcripts in zebrafish tumors	*Danio rerio*
AQUAEXCEL-2	Confinement stress Dataset	*Oncorhynchus mykiss*
GSE25584-GPL11206	Confinement stress in HR and LR trout lines	*Oncorhynchus mykiss*
GSE19170-GPL2716	Conservation genomics of Atlantic salmon	*Salmo salar*
GSE19111-GPL2716	Conservation genomics of Atlantic salmon (Year One)	*Salmo salar*
GSE19119-GPL2716	Conservation genomics of Atlantic salmon (Year Two)	*Salmo salar*
GSE20460-GPL7302	Danio spinal cord injury	*Danio rerio*
GSE20707-GPL1319	Detection of the up-regulated and down-regulated genes in stac mutant of zebrafish by cDNA microarray	*Danio rerio*
GSE23053-GPL10704	Diclofenac affects global hepatic gene expression in fish at plasma concentrations similar to human therapeutic levels	*Oncorhynchus mykiss*
AQUAEXCEL-4	Diet adipose Dataset	*Sparus aurata*
AQUAEXCEL-5	Diet liver Dataset	*Sparus aurata*
GSE34578-GPL10706	Dietary soyasaponin supplementation to pea protein concentrate reveals nutrigenomic interactions underlying enteropathy in Atlantic salmon	*Salmo salar*
GSE8309-GPL2716	Differences found in expression of cell surface & ECM components during development of the rainbow trout ovary & testis.	*Oncorhynchus mykiss*

GSE30555-GPL13225	Differences in transcription levels among wild, domesticated, and hybrid Atlantic salmon (Salmo salar) from two environments	*Salmo salar*
GSE2069-GPL1743	Differential expression under hypoxia in zebrafish	*Danio rerio*
GSE17854-GPL9117	Differential gene expression in Danio rerio during optic nerve regeneration	*Danio rerio*
GSE12516-GPL7194	Differentially expressed genes in zebrafish vascular development	*Danio rerio*
GSE8631-GPL2899	Discovery of genes associated with whirling disease infection and resistance in rainbow trout using expression profiling	*Oncorhynchus mykiss*
GSE37628-GPL15475	Does ketoprofen or diclofenac pose the lowest risk to fish?	*Oncorhynchus mykiss*
GSE16903-GPL2716	Domestication causes large-scale effects on gene expression in rainbow trout	*Oncorhynchus mykiss*
GSE16889-GPL2716	Domestication causes large-scale effects on gene expression in rainbow trout: Analysis of the brain transcriptome	*Oncorhynchus mykiss*
GSE16897-GPL2716	Domestication causes large-scale effects on gene expression in rainbow trout: Analysis of the liver transcriptome	*Oncorhynchus mykiss*
GSE16901-GPL2716	Domestication causes large-scale effects on gene expression in rainbow trout: Analysis of the muscle transcriptome	*Oncorhynchus mykiss*
GSE21914-GPL10429	Dynamic transcriptomic profiles of zebrafish gills in response to zinc	*Danio rerio*
GSE21894-GPL10429	Dynamic transcriptomic profiles of zebrafish gills in response to zinc depletion	*Danio rerio*
GSE21907-GPL10429	Dynamic transcriptomic profiles of zebrafish gills in response to zinc supplementation.	*Danio rerio*
GSE1887-GPL1516	early developmental stages of sea bream	*Sparus aurata*
GSE10981-GPL6154	Effect of dietary immunostimulation in gills and intestine of rainbow trout	*Oncorhynchus mykiss*
GSE11949-GPL6154	Effect of dietary immunostimulation in head kidney and spleen of rainbow trout	*Oncorhynchus mykiss*
GSE12961-GPL6154	Effect of dietary immunostimulation in the portals of entry of rainbow trout after LPS challenge	*Oncorhynchus mykiss*
GSE33715-GPL2716	Effect of nonylphenol on gene expression in Atlantic salmon liver, gill, hypothalamus, pituitary, and olfactory rosettes	*Salmo salar*
GSE6944-GPL3976	Effect of starvation on global gene expression and proteolysis in rainbow trout (Oncorhynchus mykiss).	*Oncorhynchus mykiss*
GSE11107-GPL1319	Effect of starvation on the transcriptomes of the brain and liver in adult female zebrafish (Danio rerio)	*Danio rerio*
GSE23157-GPL6457	Effects of diazepam on gene expression and link to physiological effects in different life stages in zebrafish Danio rerio	*Danio rerio*
GSE15216-GPL6563	Effects of haloperidol on zebrafish and fathead minnow gene expression	*Danio rerio*
GSE7853-GPL5182	Effects of hypothermia on gene expression in zebrafish gills	*Danio rerio*
GSE23156-GPL6457	Effects of PKC412 on gene expression and link to physiological effects in zebrafish Danio rerio eleuthero-embryos	*Danio rerio*
GSE14718-GPL1319	Effects of the Aromatase Inhibitor Fadrozole on Gene Expression in the Zebrafish Telencephalon	*Danio rerio*
GSE27649-GPL9663	Effects of the total replacement of fish meal and fish oil with plant protein and oil sources on the hepatic transcriptome of two European sea bass (Dicentrarchus labrax) sub-families exhibiting different growth potentials on an all plant-based diet	*Dicentrarchus labrax*
GSE5928-GPL3650	Egg quality after natural and controlled ovulation	*Oncorhynchus mykiss*

GSE38763-GPL6154	Estrogen modulates hepatic gene expression and survival of rainbow trout infected with pathogenic bacteria Yersinia ruckeri.	*Oncorhynchus mykiss*
GSE38603-GPL15678	Exercise training effects on disease resistance are dependent on training regimes and inherent swimming performance in Atlantic salmon	*Salmo salar*
GSE17655-GPL7302	Experiment 1: Developmental time curve in wild-type and MZspg embryos	*Danio rerio*
GSE17659-GPL7302	Experiment 2: Pou5f1 and Sox2 overexpression experiments with or without protein synthesis inhibition	*Danio rerio*
GSE17656-GPL7302	Experiment 3: Comparison of MZspg and Mspg transcriptomes	*Danio rerio*
GSE17657-GPL1319	Experiment 4: Affymetrix validation array	*Danio rerio*
GSE24527-GPL1319	Expression analysis of 24hpf zebrafish embryos treated with Leflunomide 6.5uM	*Danio rerio*
GSE26372-GPL10392	Expression analysis of melanoma harvested after GFP or SETDB1 expression	*Danio rerio*
GSE21505-GPL10392	Expression analysis of melanoma harvested from GFP versus SETDB1 transgenic zebrafish (Danio rerio)	*Danio rerio*
GSE24529-GPL1319	Expression analysis of transgenic embryos carrying the mitf-BRAFV600E allele in the presence or absence of p53 function	*Danio rerio*
GSE28131-GPL13318	Expression Analysis of Trimethyltin Chlorides (TMT) Impact on Embryonic Development	*Danio rerio*
GSE24528-GPL1319	Expression analysis of zebrafish melanoma and skin from the mitf-BRAFV600E;p53-/- line	*Danio rerio*
GSE19955-GPL1319	Expression data comparing wild-type and spt mutant zebrafish tissues at two developmental time points.	*Danio rerio*
GSE5586-GPL1319	Expression data from egy wildtype and mutant embryo comparison	*Danio rerio*
GSE8800-GPL1319	Expression data from embryos injected with DrC1q-like morpholino and control morpholino	*Danio rerio*
GSE27569-GPL1319	Expression data from zebrafish depleted of Esco2	*Danio rerio*
GSE18795-GPL1319	Expression data from zebrafish embryos homozygous mutant for the cohesin subunit Rad21	*Danio rerio*
GSE13196-GPL1319	Expression data from zebrafish pineal gland	*Danio rerio*
GSE12116-GPL6467	Expression profiles in two early developmental stages of Sparus aurata	*Sparus aurata*
GSE16029-GPL3650	Expression profiling of rainbow trout testicular development and spermatogenesis	*Oncorhynchus mykiss*
GSE13482-GPL7556	Expression profiling of zebrafish sox9 mutants reveals that Sox9 is required for retinal differentiation	*Danio rerio*
GSE12189-GPL1319	FACS-Assisted Microarray Profiling Implicates Novel Genes and Pathways in Zebrafish Gastrointestinal Tract Development	*Danio rerio*
GSE8874-GPL1319	Factorial Microarray Analysis of Zebrafish Retinal Development	*Danio rerio*
GSE13348-GPL1319	Foggy mutant: brain (Guo-1R01NS042626-01A2)	*Danio rerio*
GSE31871-GPL14375	Gender specific comparisons of gene expression during Zebrafish pectoral fin regeneration	*Danio rerio*
GSE8724-GPL1319	Gene expression analysis in the zebrafish embryos silenced by zfPGRP-SC	*Danio rerio*
GSE18566-GPL6563	Gene expression analysis of diet induced obesity model zebrafish	*Danio rerio*
GSE17773-GPL6457	Gene expression analysis of zebrafish embryos depleted of arrb1 and/or arrb2 at 12 hpf	*Danio rerio*
GSE28812-GPL13443	Gene expression based on an oligonucleotide microarray for Dicentrarchus labrax	*Dicentrarchus labrax*
GSE22662-GPL2878	Gene expression changes in the female zebrafish (Danio rerio) brain in response to acute exposure to methylmercury	*Danio rerio*
GSE11700-GPL5573	Gene expression during hyper and hypoosmotic stress adaptation in Gillichthys mirabilis	*Gillichthys mirabilis*
GSE5813-GPL2096	Gene expression during tumor enhancement by 3,3'-diindolylmethane in rainbow trout	*Oncorhynchus mykiss*

GSE5643-GPL2096	Gene expression during tumor enhancement by 3,3'-diindolylmethane in rainbow trout: HCC tumor samples	*Oncorhynchus mykiss*
GSE5644-GPL2096	Gene expression during tumor enhancement by 3,3'-diindolylmethane in rainbow trout: Timecourse	*Oncorhynchus mykiss*
GSE36072-GPL10706	Gene expression in Atlantic salmon skin in response to infection with the parasitic copepod Lepeophtheirus salmonis, cortisol implant, and their combination	*Salmo salar*
GSE1995-GPL1319	Gene expression in foggy mutant. Guo-1R01NS042626-01A2	*Danio rerio*
GSE6142-GPL4481	Gene expression in homozygous mbl/axin1 zebrafish	*Danio rerio*
GSE18389-GPL6154	Gene expression in the Atlantic salmon adipose-derived stromal-vascular fraction during differentiation into adipocytes	*Salmo salar*
GSE2686-GPL2096	Gene expression in trout hepatocellular carcinoma	*Oncorhynchus mykiss*
GSE20137-GPL9998	Gene expression in unfertilized eggs and the MBT stage of zebrafish embryos	*Danio rerio*
GSE7658-GPL1319	Gene Expression Profile of Hematopoietic Stem Cells during Zebrafish Development	*Danio rerio*
GSE12955-GPL1319	Gene expression profile of zebrafish kidney side population (SP) cells	*Danio rerio*
GSE19049-GPL6563	Gene expression profiles after infection of zebrafish with viral haemorrhagic septicemia rhabdovirus (VHSV)	*Danio rerio*
GSE12140-GPL1319	Gene expression profiles in zebrafish brain after acute exposure to domoic acid at symptomatic and asymptomatic doses	*Danio rerio*
GSE3303-GPL1319	Gene Expression Profiles of Intact and Regenerating Zebrafish Retina	*Danio rerio*
GSE3522-GPL2899	Gene Expression Profiling Following DNA Vaccination of Rainbow Trout against Infectious Hematopoietic Necrosis Virus	*Oncorhynchus mykiss*
GSE6228-GPL4518	Gene expression profiling in zebrafish embryos exposed to 3,4-dichloroaniline (3,4-DCA)	*Danio rerio*
GSE36475-GPL10679	Gene expression profiling of soft and firm Atlantic salmon fillet	*Salmo salar*
GSE5048-GPL1319	Gene Expression Profiling of Zebrafish Embryonic Retinal Pigment Epithelium in vivo.	*Danio rerio*
GSE19298-GPL1319	Gene expression timecourse in zebrafish whole eye in response to optic nerve crush	*Danio rerio*
GSE14495-GPL1319	Gene profiling of Müller glia during early stages of zebrafish photoreceptor regeneration	*Danio rerio*
GSE26609-GPL7302	Genes for embryo development are packaged in blocks of multivalent chromatin in zebrafish sperm	*Danio rerio*
GSE19630-GPL8904	Genetic markers of the immune response of Atlantic salmon (Salmo salar) to Infectious Salmon Anemia Virus (ISAV)	*Salmo salar*
E-TABM-1089-A-MEXP-1930	Genotype-specific responses in hepatic lipid metabolism to complete dietary fish oil replacement by vegetable oil in Atlantic salmon	*Salmo salar*
E-TABM-1173-A-MEXP-1930	Genotype-specific responses in intestinal lipid metabolism to complete dietary fish oil replacement by vegetable oil in Atlantic salmon	*Salmo salar*
AQUAEXCEL-3	Gill cells culture Dataset	*Oncorhynchus mykiss*
AQUAEXCEL-11	Gill salinity Dataset	*Oncorhynchus mykiss*
GSE12909-GPL7338	Global Expression Analysis of Vasculogenesis Induction by Zebrafish Ets1-Related Protein	*Danio rerio*
GSE9595-GPL2716	Global gene expresssion profiling the gills of amoebic gill disease (AGD) affected Atlantic salmon (Salmo salar)	*Salmo salar*
GSE37574-GPL15475	Global hepatic gene expression in rainbow trout exposed to sewage effluents	*Oncorhynchus mykiss*

AQUAEXCEL-8	Heart Dataset	*Sparus aurata*
GSE9870-GPL5573	Heat stress response in Gillichthys mirabilis	*Gillichthys mirabilis*
GSE19483-GPL2716	Hepatic Gene Expression in Rainbow Trout (Oncorhynchus mykiss) Exposed to Different Hydrocarbon Mixtures	*Oncorhynchus mykiss*
GSE7671-GPL3713	Hepatic transcriptome response to glucocorticoid receptor activation in rainbow trout.	*Oncorhynchus mykiss*
E-TABM-1204-A-MEXP-2065	Hepatic transcriptomic analysis of inter-family variability in flesh n-3 long-chain polyunsaturated fatty acid content in Atlantic salmon	*Salmo salar*
GSE8826-GPL2716	High gene expression of inflammatory markers and IL-17A in Atlantic salmon vaccinated with oil-adjuvanted vaccines	*Salmo salar*
GSE10951-GPL6563	Hypoxia alters gene expression in the gonads of zebrafish	*Danio rerio*
GSE24840-GPL11077	Identification and developmental expression of the full complement of cytochrome P450 genes in zebrafish	*Danio rerio*
GSE33257-GPL10770	Identification of a responsive gene set to evaluate the potential impact of seismic exposure on Atlantic salmon (Salmo salar) inner ear	*Salmo salar*
GSE8226-GPL5478	Identification of a transcriptional fingerprint of estrogen exposure in rainbow trout liver	*Oncorhynchus mykiss*
GSE16030-GPL3650	Identification of androgen-responsive genes in fish testis	*Oncorhynchus mykiss*
GSE8076-GPL4609	Identification of differentially-expressed genes between FoxH1 morpholino and control in zebrafish embryos.	*Danio rerio*
GSE12857-GPL7343	Identification of direct T-box target genes in the developing zebrafish mesoderm	*Danio rerio*
GSE5199-GPL3721	Identification of downstream targets of zebrafish Hoxb1a	*Danio rerio*
GSE30632-GPL13908	Identification of Hoxb1b regulated genes in zebrafish embryos	*Danio rerio*
GSE8654-GPL4609	Identification of mesendoderm precursor- and neurectoderm precursor-enriched genes in Zebrafish embryos	*Danio rerio*
GSE25042-GPL11151	Identification of novel genes associated with molecular sex differentiation in the embryonic gonads of rainbow trout (Oncorhynchus mykiss)	*Oncorhynchus mykiss*
GSE6853-GPL4375	Identification of sexually dimorphic gene expression in the brain of adult zebrafish (Danio rerio)	*Danio rerio*
GSE13068-GPL1319	Identification of the molecular signatures integral to regenerating photoreceptors in the retina of the zebrafish	*Danio rerio*
GSE25440-GPL11206	Individual variation in confinement response at 168h	*Oncorhynchus mykiss*
GSE9260-GPL3721	Inflammation and degeneration of the olfactory epithelium in an immuno-deficient zebrafish	*Danio rerio*
GSE10272-GPL6155	Inflammatory response of trout head kidney to in vivo challenge with IHN virus and LPS	*Oncorhynchus mykiss*
GSE17949-GPL1319	Integrated cell-to-cell signaling networks regulate vertebrate axis formation and left-right asymmetry	*Danio rerio*
AQUAEXCEL-6	Intestine Dataset	*Sparus aurata*
GSE12991-GPL1319	Isolation of single miRNA-expressing cells from zebrafish embryos	*Danio rerio*
GSE23613-GPL3713	Juvenile rainbow trout exposed in situ at site receiving different concentrations of municipal wastewater effluent (MWWE) and an upstream reference site	*Oncorhynchus mykiss*
GSE17711-GPL1319	Lack of de novo phosphatidylinositol synthesis leads to endoplasmic reticulum stress and hepatic steatosis in cdipt-deficient zebrafish	*Danio rerio*

GSE2151-GPL1793	Large-scale temporal gene expression profiling during gonadal differentiation and early gametogenesis in rainbow-trout	*Oncorhynchus mykiss*
E-MEXP-2415-A-MEXP-1717	Lgl2 executes its function as a tumor suppressor by regulating ErbB signaling in the zebrafish epidermis	*Danio rerio*
GSE12031-GPL3650	Livers from lean or fat muscle lines fed low or high lipid diets	*Oncorhynchus mykiss*
GSE2264-GPL1212	M74 disorder in Baltic salmon	*Salmo salar*
GSE13197-GPL6154	Macrophages stimulated with LPS and Poly (I:C)	*Oncorhynchus mykiss*
GSE19206-GPL7735	Macrophage-specific gene functions in Spi1-directed innate immunity	*Danio rerio*
GSE23872-GPL10816	Mapping of H3K4 and H3K27 trimethylation in zebrafish cells	*Danio rerio*
GSE23679-GPL10816	Mapping of H3K4 and H3K27 trimethylation in zebrafish cells (Gene expression)	*Danio rerio*
GSE7837-GPL2096	Mechanism for hepatic tumor promotion by PFOA in rainbow trout	*Oncorhynchus mykiss*
GSE18861-GPL2715	Mercury-Induced Hepatotoxicity in Zebrafish	*Danio rerio*
GSE7220-GPL3548	Microarray analysis in the zebrafish liver and telencephalon after exposure to low concentration of 17a-EE2	*Danio rerio*
GSE28310-GPL6260	Microarray analysis of differential utilization of plant based diets by rainbow trout	*Oncorhynchus mykiss*
GSE30782-GPL13442	Microarray analysis of transcripts in the liver of gilthead sea bream with high plasma cortisol levels induced by slow-release cortisol implants	*Sparus aurata*
GSE4787-GPL2899	Microarray gene expression analysis in atrophying rainbow trout muscle: An unique non-mammalian muscle degradation model	*Oncorhynchus mykiss*
GSE12214-GPL1319	Microcystin Genomic Effects on Zebrafish Larvae	*Danio rerio*
GSE6063-GPL4375	Molecular basis of gender and reproductive status in breeding zebrafish	*Danio rerio*
GSE3519-GPL2715	Molecular Conservation of Zebrafish and Human Liver Tumors.	*Danio rerio*
GSE25617-GPL4021	Molecular dissection of the migrating posterior lateral line primordium during early development in zebrafish	*Danio rerio*
GSE4859-GPL1319	Molecular targets of 2,3,7,8-tetrachlorodibenzo-p-dioxin (TCDD) within the zebrafish ovary	*Danio rerio*
GSE20884-GPL10182	Morphological and molecular evidence that the zebrafish intestine is organized into a small and large intestine	*Danio rerio*
AQUAEXCEL-7	Muscle Dataset	*Sparus aurata*
GSE14782-GPL7735	Mycobacterium marinum chronic infection of adult zebrafish	*Danio rerio*
GSE1894-GPL1319	nck2 vs. wt morpholino	*Danio rerio*
GSE19478-GPL2716	Normal and shortened photoperiods in liver, ovary, and pituitarty	*Oncorhynchus mykiss*
GSE28610-GPL13442	Oligonucleotide microarray for Sparus aurata	*Sparus aurata*
GSE21756-GPL5182	Over-expression of Akt1 Induces Skin Hypertrophy and Generates an Obesity Model in Zebrafish	*Danio rerio*
GSE8656-GPL5675	Pair wise comparison between STD-MO and klf4-MO embryos	*Danio rerio*
AQUAEXCEL-14	PEPPA Dataset	*Oncorhynchus mykiss*
GSE15124-GPL8254	Pharmaceutical industry effluent diluted 1:500 affects gene expression, CYP1A activity and plasma phosphate in fish	*Oncorhynchus mykiss*
AQUAEXCEL-1	PNA-PVC Dataset	*Oncorhynchus mykiss*
GSE17667-GPL1319	Pou5f1 transcription targets in zebrafish	*Danio rerio*
GSE17667-GPL7302	Pou5f1 transcription targets in zebrafish	*Danio rerio*

GSE28199-GPL1319	prdm1a mutant vs. wild type	*Danio rerio*
GSE4871-GPL3650	Preovulatory ovary	*Oncorhynchus mykiss*
GSE3475-GPL2844	Profiling of Salmo salar in two Atlantic salmon types, a wild type versus transgenic.	*Salmo salar*
GSE23315-GPL7301	Quantitative analysis of thyroid response in zebrafish embryos	*Danio rerio*
GSE29308-GPL13537	Raf/MEK signatures in zebrafish liver cells	*Danio rerio*
AQUAEXCEL-15	RAFOA Dataset	*Oncorhynchus mykiss*
GSE22379-GPL6154	Rainbow trout erythrocytes stimulated with LPS and Poly(I:C)	*Oncorhynchus mykiss*
GSE21084-GPL2716	Rainbow trout red blood cells (RBCs): Control vs Heat shock, repeated samples from individuals	*Oncorhynchus mykiss*
GSE6841-GPL3650	Recovery growth	*Oncorhynchus mykiss*
AQUAEXCEL-9	Red muscle Dataset	*Sparus aurata*
GSE12039-GPL1319	Regulation of endothelial gene expression by miR-126 in human and zebrafish	*Danio rerio*
GSE12012-GPL1319	Regulation of zebrafish endothelial gene expression by miR-126	*Danio rerio*
GSE1376-GPL1212	Response to stress in brain and kidney	*Oncorhynchus mykiss*
GSE27013-GPL10705	Responses to ectoparasite salmon louse (Lepeophtheirus salmonis) in Atlantic salmon	*Salmo salar*
GSE27013-GPL10706	Responses to ectoparasite salmon louse (Lepeophtheirus salmonis) in Atlantic salmon	*Salmo salar*
GSE26981-GPL10705	Responses to ectoparasite salmon louse (Lepeophtheirus salmonis) in skin of Atlantic salmon	*Salmo salar*
GSE26984-GPL10706	Responses to ectoparasite salmon louse (Lepeophtheirus salmonis) in spleen of Atlantic salmon	*Salmo salar*
GSE8522-GPL2715	RNA from 3 d and 2 d old embryos of mibta52b, mibm132 and mibtfi91, and RNA from 3 d, 2d and 1 d old embryos of mibta52b	*Danio rerio*
AQUAEXCEL-16	Salinity Dataset 1	*Oncorhynchus mykiss*
AQUAEXCEL-17	Salinity Dataset 2	*Oncorhynchus mykiss*
AQUAEXCEL-18	Salinity Dataset 3	*Oncorhynchus mykiss*
AQUAEXCEL-16-17	Salinity Datasets 1-2	*Oncorhynchus mykiss*
GSE8526-GPL2844	Salmon Macrophage early response to Aeromonas salmonicida	*Salmo salar*
GSE13994-GPL7735	Salmonella typhimurium infection of zebrafish embryo	*Danio rerio*
GSE6924-GPL2899	Salmonid host response to Hematopoietic Necrosis virus: cellular receptors, viral control and novel pathways of defence	*Salmo salar*
GSE6924-GPL3976	Salmonid host response to Hematopoietic Necrosis virus: cellular receptors, viral control and novel pathways of defence	*Salmo salar*
GSE19646-GPL10126	SEA BREAM PATH_INTEST	*Sparus aurata*
GSE16633-GPL8467	SEA BREAM_CONFINEMENT	*Sparus aurata*
GSE14979-GPL1319	Sex- and gonad-biased gene expression in zebrafish	*Danio rerio*
GSE8856-GPL1319	Sexual dimorphism in the zebrafish hepatic transcriptome and response to dietary carbohydrate	*Danio rerio*
GSE8285-GPL3976	Short-term growth hormone treatment on the liver and muscle transcriptome in rainbow trout (Oncorhynchus mykiss)	*Oncorhynchus mykiss*
GSE30717-GPL13926	Skin healing and scale regeneration in fed and unfed sea bream, Sparus auratus	*Sparus aurata*
GSE14861-GPL6563	Small fish comp tox ZF haloperidol 96 h ovary	*Danio rerio*
GSE15796-GPL1319	Spatiotemporal Analysis of Transcriptome in the paraxial mesoderm of zebrafish embryos	*Danio rerio*

GSE15328-GPL7735	Specificity of the zebrafish host transcriptome response to acute and chronic mycobacterial infection	*Danio rerio*
GSE21077-GPL5182	Stage-specific expression of TNFa regulates bad/bid-mediated apoptosis and RIP1/ROS-mediated secondary necrosis in Birnavirus-infected fish cells	*Danio rerio*
GSE20849-GPL10169	Steady State Thermal Acclimation in the Eurythermal Goby fish, Gillichthys mirabilis	*Gillichthys mirabilis*
GSE2064-GPL1516	stress response	*Sparus aurata*
GSE20131-GPL6154	Swimming down-regulates ovarian transcriptomic response of rainbow trout Oncorhynchus mykiss	*Oncorhynchus mykiss*
GSE12118-GPL6467	Technical replicates to determine array-to-array reproducibility.	*Sparus aurata*
GSE2277-GPL1212	Temperature acclimation in rainbow trout heart	*Oncorhynchus mykiss*
GSE17083-GPL7301	Temperature probe selection experiment for custom array production	*Danio rerio*
GSE17086-GPL7301	Temperature validation experiment for custom array production	*Danio rerio*
GSE19489-GPL2716	Temporal patterns in the transcriptomic response of rainbow trout, Oncorhynchus mykiss, to crude oil	*Oncorhynchus mykiss*
GSE25305-GPL10679	Tetradecylthioacetic acid effect on heart ventricle	*Salmo salar*
GSE25305-GPL10705	Tetradecylthioacetic acid effect on heart ventricle	*Salmo salar*
GSE13999-GPL1319	The cellular expression of midkine-a and midkine-b during retinal development and photoreceptor regeneration	*Danio rerio*
GSE16740-GPL1319	The effect of cardiac troponin T2 knockdown on gene expression in zebrafish embryos	*Danio rerio*
GSE4790-GPL2899	The effects of chronic immune stimulation on muscle growth in rainbow trout	*Oncorhynchus mykiss*
GSE6127-GPL1319	The expression of Spt5 targeted genes	*Danio rerio*
GSE8428-GPL1319	The expression profiles of control embryos and pbx2-MO;pbx4-MO embryos at 10 somites and at 18 somites.	*Danio rerio*
GSE21134-GPL2878	The gene profile of zebrafish guanine binding protein-like 2 (Gnl2) mutant embryos versus wild-type embryos at 22 hours post-fertilization	*Danio rerio*
GSE27299-GPL10532	The impact of chronic temperature elevation on the spleen anti-viral transcriptomic response in Atlantic cod (Gadus morhua)	*Gadus morhua*
GSE24934-GPL6457	The knockdown of the maternal estrogen receptor-ß2 mRNA (ers2a) affects embryo transcript contents and larval development in zebrafish	*Danio rerio*
GSE13771-GPL1319	The role of ERbeta2 in zebrafish neuromasts development	*Danio rerio*
GSE13157-GPL1319	The role of ERbeta2 in zebrafish neuromasts development 15uM	*Danio rerio*
GSE13158-GPL1319	The role of ERbeta2 in zebrafish neuromasts development 50uM	*Danio rerio*
GSE22312-GPL10532	The study of Atlantic cod (Gadus morhua) spleen global gene expression response to intraperitoneal injection with formalin-killed atypical Aeromonas salmonicida.	*Gadus morhua*
GSE14399-GPL7801	The use of zebrafish reward mutants to search for novel transcripts mediating the behavioral effects of amphetamine	*Danio rerio*
GSE4585-GPL1319	The zebrafish runzel mutant results in a novel muscular dystrophy phenotype due to a titin mutation	*Danio rerio*
GSE25473-GPL11206	Time course study of confinement stress in HR and LR trout lines	*Oncorhynchus mykiss*
GSE6886-GPL3713	Tissue Contaminants and Associated Transcriptional Response in Trout Liver from High Elevation Lakes of Washington	*Oncorhynchus mykiss*
GSE3324-GPL966	Toxicogenomic profiling of trout tumor promoters	*Oncorhynchus mykiss*

GSE6416-GPL2716	Toxicogenomic responses in rainbow trout hepatocytes exposed to model chemicals and a synthetic mixture	*Oncorhynchus mykiss*
GSE20310-GPL10042	Traf6 function in the innate immune response of zebrafish embryos	*Danio rerio*
GSE3048-GPL2715	Trancriptome Kinetics of Arsenic-induced Adaptive Response in Zebrafish Liver.	*Danio rerio*
GSE31085-GPL5478	Transcript profiles of PFAAs in trout liver	*Oncorhynchus mykiss*
GSE23381-GPL1319	Transcription profile of zebrafish hand2 (hanS6 allele) mutant embryos at 19hpf	*Danio rerio*
E-TABM-1056-A-MEXP-804	Transcription profiling by array of Atlantic salmon fed genetically modified Bt-maize or non-modified parental maize	*Salmo salar*
E-TABM-1000-A-MEXP-664	Transcription profiling by array of Atlantic salmon head kidney cells infected with infectious pancreatic necrosis virus	*Salmo salar*
E-TABM-1060-A-MEXP-1790	Transcription profiling by array of Atlantic salmon infected with salmoin alphavirus	*Salmo salar*
E-TABM-955-A-MEXP-1790	Transcription profiling by array of Atlantic salmon liver from fish exhibiting high and low flesh n-3LC-PUFA levels at harvest	*Salmo salar*
E-TABM-1065-A-MEXP-1790	Transcription profiling by array of salmon parr brain after exposure to the carbamazepine	*Salmo salar*
E-MEXP-818-A-AFFY-38	Transcription profiling of animal caps from Danio rerio embryos expressing GFP or vhnf1 and treated with FGF8 or BSA protein	*Danio rerio*
E-MEXP-1023-A-MEXP-664	Transcription profiling of Atlantic salmon cell line SHK-1 exposed to interferon type 1 and interferon gamma for 6 or 24 hours	*Salmo salar*
E-TABM-678-A-MEXP-804	Transcription profiling of Atlantic salmon fed with a low, medium or high histidine diet	*Salmo salar*
E-TABM-478-A-MEXP-664	Transcription profiling of Atlantic salmon following dietary substitution of fish oil with vegetable oils	*Salmo salar*
E-MEXP-1301-A-AFFY-38	Transcription profiling of brain from zebrafish treated with ethanol or nicotine suggests conservation of neuro-adaptation pathways	*Danio rerio*
E-MEXP-2381-A-AFFY-38	Transcription profiling of Danio rerio (zebrafish) RPL11 mutant vs siblings	*Danio rerio*
E-MEXP-2287-A-MEXP-1580	Transcription profiling of Danio rerio livers following chronic waterborne copper exposure	*Danio rerio*
E-MEXP-2288-A-AFFY-38	Transcription profiling of Danio rerio livers following exposure to combinations of copper, sodium and calcium	*Danio rerio*
E-TABM-552-A-MEXP-1396	Transcription profiling of dorsal epaxial fast muscle from zebra fish at developmental stages where myotubes are still actively recruited (M+ stage) and where myotube production has ceased (M- stage)	*Danio rerio*
E-MEXP-1163-A-AGIL-30	Transcription profiling of ERK1 and ERK2 knockdown in zebrafish embryos at blastula stage	*Danio rerio*
E-TABM-1040-A-MEXP-1865	Transcription profiling of Gadus morhua pituitary gland, pylorus, spleen and testis to validate the IMR Atlantic Cod 16k cDNA array	*Gadus morhua*
E-MEXP-1396-A-MEXP-664	Transcription profiling of gill from ameobic gill disease resistant and susceptible Atlantic salmon	*Salmo salar*
E-MEXP-1267-A-MEXP-664	Transcription profiling of gill, kidney and brain from Atlantic salmon at different developmental stages to identify genes involved in freshwater to salt water adaptation	*Salmo salar*
E-MEXP-1286-A-MEXP-664	Transcription profiling of gill, liver and kidney from amoebic gill disease infected and disease-free Atlantic salmon	*Salmo salar*
E-MEXP-1149-A-MEXP-804	Transcription profiling of liver from rainbow trout treated with estrogen to identify biomarkers of estrogenic compound exposure	*Oncorhynchus mykiss*

E-MEXP-1683-A-MEXP-1374	Transcription profiling of male zebra fish exposed to E2 and liver from non-vitellogenic and vitellogenic females to identify genes associated with vitellogenisis	*Danio rerio*
E-MEXP-1593-A-AGIL-30	Transcription profiling of rac1 knock-down zebrafish embryos	*Danio rerio*
E-MEXP-622-A-MEXP-309	Transcription profiling of rainbow trout liver in response to standardized handling stress	*Oncorhynchus mykiss*
E-MEXP-946-A-MEXP-619	Transcription profiling of Salmo salar (Salmon) hepatocytes treated with DMSO (control), nonylphenol and 3,3,4,4-tetrachlorobiphenyl to identify interactions between estrogen and aryl hydrocarbon receptor signalling pathways	*Salmo salar*
E-MEXP-181-A-MEXP-110	Transcription profiling of sea bream during early development	*Sparus aurata*
E-MEXP-737-A-AFFY-38	Transcription profiling of two 24 hour old zebrafish embryos from the Tuebingen line	*Danio rerio*
E-MEXP-1685-A-MEXP-1048	Transcription profiling of zebra fish liver after water-borne exposure to polycyclic aromatic hydrocarbons and alkylphenols	*Danio rerio*
E-MEXP-775-A-MEXP-536	Transcription profiling of zebra fish squint mutant and wild type embryos following a temperature shift in development to investigate environmental and genetic modifiers of squint penetrance	*Danio rerio*
E-MEXP-405-A-AFFY-38	Transcription profiling of zebrafish at the late stage of chronic tuberculosis due to Mycobacterium marinum infection	*Danio rerio*
E-MEXP-2215-A-AFFY-38	Transcription profiling of zebrafish cls/sox10 mutants at 4dpf compared to their wild type siblings at 4 day identifies lndc1 as a novel factor in Schwann cell development	*Danio rerio*
E-TABM-33-A-AFFY-38	Transcription profiling of zebrafish development	*Danio rerio*
E-MEXP-1879-A-MEXP-1050	Transcription profiling of zebrafish embryos injected with Ofd1 morphlino compared to wild type	*Danio rerio*
E-TABM-354-A-AFFY-38	Transcription profiling of zebrafish embryos with dpf3 knocked down for morpholino	*Danio rerio*
E-MEXP-171-A-AFFY-38	Transcription profiling of zebrafish germ layer morphogenesis	*Danio rerio*
E-TABM-105-A-AFFY-38	Transcription profiling of zebrafish livers following exposure to 17 alpha-ethynylestradiol (EE2) at 0, 15, 40, or 100 ng/L	*Danio rerio*
E-MEXP-1272-A-MEXP-838	Transcription profiling of zebrafish ovary, testis, brain, kidney and whole body to identify gonad-expressed genes and their expression in various organs	*Danio rerio*
E-MEXP-2365-A-MEXP-1048	Transcription profiling of zebrafish wild type and prion protein prp2-morphants injected early embryos.	*Danio rerio*
E-MEXP-736-A-AFFY-38	Transcription profiling of zebrafish ZF4 and PAC2 cell lines cultured in medium with or without FCS	*Danio rerio*
E-MEXP-1239-A-AFFY-38	Transcription profiling time series of Danio rerio heart regeneration	*Danio rerio*
E-MEXP-758-A-AFFY-38	Transcription profiling time series of zebrafish hearts treated with dioxin (TCDD)	*Danio rerio*
GSE20179-GPL6457	Transcriptional profiling of embryonic zebrafish expressing a mutant TNNT2	*Danio rerio*
GSE12655-GPL7244	Transcriptional profiling of rag1 deficient (rag1-/-) and rag1 heterozygous (rag1+/-) zebrafish kidney and intestine	*Danio rerio*
E-MEXP-3062-A-MEXP-1048	Transcriptional Regulation in liver Associated with Developmental and Reproductive Effects in Female Zebrafish Exposed to Natural Mixtures of Persistent Organic Pollutants from Lake Mjosa	*Danio rerio*
E-MEXP-3061-A-MEXP-1048	Transcriptional Regulation in Testis Associated with Developmental and Reproductive Effects in Male Zebrafish Exposed to Natural Mixtures of Persistent Organic Pollutants from Mjosa Lake	*Danio rerio*
GSE28357-GPL7303	Transcriptional response of Atlantic salmon (Salmo salar) after primary versus secondary exposure to Infectious Salmon Anemia Virus (ISAV)	*Salmo salar*

E-TABM-449-A-MEXP-664	Transcriptional response of Atlantic salmon (Salmo salar) to fish oil vs vegetable oil based diets	*Salmo salar*
GSE13050-GPL3209	Transcriptome Analysis of the Zebrafish Mind Bomb Mutant	*Danio rerio*
GSE13371-GPL1319	Transcriptome analysis of the zebrafish pineal gland	*Danio rerio*
GSE19754-GPL1319	Transcriptome analysis of zebrafish mononuclear myogenic cells (zMNCs) during myogenic differentiation	*Danio rerio*
GSE8651-GPL5692	Transcriptome analysis of zebrafish yquem/urod mutant	*Danio rerio*
GSE13570-GPL2716	Transcriptome profiling of embryonic development rate in rainbow trout advance backcross introgression lines	*Oncorhynchus mykiss*
GSE28843-GPL10679	Transcriptome profiling of immune responses to cardiomyopathy syndrome (CMS) in Atlantic salmon	*Salmo salar*
GSE28843-GPL10705	Transcriptome profiling of immune responses to cardiomyopathy syndrome (CMS) in Atlantic salmon	*Salmo salar*
GSE11160-GPL6154	Transcriptomic analysis of responses to infectious salmon anemia virus infection in macrophage-like cells	*Salmo salar*
GSE29669-GPL7302	Transcriptomic analysis of the zebrafish inner ear points to growth hormone mediated regeneration following acoustic trauma	*Danio rerio*
E-TABM-1207-A-MEXP-2065	Transcriptomic and physiological responses to fishmeal substitution with plant proteins in formulated feed in farmed Atlantic salmon (Salmo salar)	*Salmo salar*
GSE36339-GPL6154	Transcriptomic response of skeletal muscle to lipopolysaccharide in the gilthead seabream (Sparus aurata)	*Sparus aurata*
GSE22330-GPL6154	Trout macrophages: Control vs. Escherichia coli PGNs from strains O111:B4 and K12	*Oncorhynchus mykiss*
GSE16577-GPL3650	Trout_Muscle_diet&selection	*Oncorhynchus mykiss*
GSE36332-GPL13225	Vaccination against yersiniosis induces a specific gill transcriptome biosignature in Atlantic salmon	*Salmo salar*
E-MEXP-2948-A-MEXP-1926	VM-zfIFNg	*Danio rerio*
AQUAEXCEL-10	White muscle Dataset	*Sparus aurata*
GSE20424-GPL10074	Zebrafish (Danio rerio) 72hpf, WT control vs. MO-Prpf31 injected	*Danio rerio*
GSE12826-GPL1319	Zebrafish 24hpf mutant sk8 gene expression	*Danio rerio*
GSE26707-GPL7735	Zebrafish 27hpf embryos: hdac1 mutant (hi1618) vs sibling	*Danio rerio*
GSE16264-GPL1319	Zebrafish embryos treated with Retinoic Acid or Retinoic acid antagonist during gastrulation and early somitogenesis.	*Danio rerio*
GSE18522-GPL7302	Zebrafish embryos: Control vs. 5-aza-2'-deoxycytidine treated	*Danio rerio*
GSE21680-GPL10387	Zebrafish embryos: exposure to 3,4-dichloraniline, 2,4-dichlorophenol, pentachlorophenol, and cadmium chloride	*Danio rerio*
GSE26708-GPL7735	Zebrafish embryos: hdac1 Morphants vs Standard control morphants	*Danio rerio*
GSE26709-GPL7735	Zebrafish embryos: hdac1 Morphants vs Standard control morphants at 12, 18 and 27 hpf	*Danio rerio*
GSE26710-GPL7735	Zebrafish hdac1 mutant and morphant embryos	*Danio rerio*
GSE17993-GPL1319	Zebrafish heart regeneration	*Danio rerio*
GSE4989-GPL1319	Zebrafish Hypoxia study Heart array	*Danio rerio*
E-MTAB-381-A-AFFY-38	Zebrafish Light Pulse	*Danio rerio*
GSE29307-GPL13537	zebrafish liver tumor signatures	*Danio rerio*
GSE29351-GPL13537	Zebrafish liver tumors	*Danio rerio*
GSE4201-GPL1319	Zebrafish microRNA miR-430 promotes deadenylation and clearance of maternal mRNAs	*Danio rerio*
GSE16857-GPL1319	Zebrafish response to microbiota	*Danio rerio*

GSE8327-GPL1319	Zebrafish response to Mycobacterium marinum infection (Affymetrix series)	*Danio rerio*
GSE8846-GPL5720	Zebrafish response to Mycobacterium marinum infection (Compugen series)	*Danio rerio*
GSE14866-GPL6563	Zebrafish von Hippel-Lindau (vhl) tumor suppressor mutants compared to siblings at 7 dpf	*Danio rerio*
GSE27707-GPL2715	Zebrafish: Estrogen induced gene expression	*Danio rerio*

Supplemental table A2.

Gene Name	Fold-change	Gene Name	Fold-change
14-3-3 protein epsilon	-1.43	Guanidinoacetate N-methyltransferase	1.73
26S proteasome complex subunit DSS1	-1.49	H2A histone member Y	-1.72
26S protease regulatory subunit 6A	-1.67	Haloacid dehalogenase-like hydrolase domain-containing protein 1A	-1.92
26S protease regulatory subunit S10B	-2.00	Heparin-binding EGF-like growth factor	1.73
26S proteasome non-ATPase regulatory subunit 14	-1.99	Histone	-2.37
4SNc-Tudor domain protein short form	1.90	HNI male sex-determining protein (DMRT1Y)	1.86
60S ribosomal export protein NMD3	1.81	Importin 7	1.41
60S ribosomal protein l37	1.90	Importin 9	2.03
60S ribosomal protein l9	1.41	Inorganic pyrophosphatase	-2.04
ADP-ribosylation factor-like 6 interacting protein	-3.02	Inositol -1(or 4)-monophosphatase 1	-2.14
Alpha-n-acetylgalactosaminidase	-1.30	Integrin alpha-6	2.16
Aminopeptidase-like 1	-1.74	Isochorismatase domain-containing protein 2	1.58
AP-4 complex subunit sigma-1	-1.36	Isopentenyl-diphosphate delta-isomerase 1	-1.90
APEX nuclease (multifunctional DNA repair enzyme)	-2.32	KIAA1143 homolog	1.54
Basic transcription factor 3	1.50	Laminin alpha 4	1.61
Beta-galactosidase	-3.77	Leukotriene A-4 hydrolase	-1.95
BolA-like protein 2	-1.82	LIN-52 homolog	1.57
C2orf76 protein	-1.88	Makorin-1	3.25
Calpain 3	-2.08	MAP microtubule affinity-regulating kinase 3	1.47
Calpastatin	2.05	Methyltransferase like 11A	-1.74
Capping protein muscle Z-line alpha 1	-1.73	Mitogen-activated protein kinase 6	-1.65
Capping protein muscle Z-line alpha 2	-1.43	Muscle specific RING finger protein 1-like	-1.48
Carbonic anhydrase	-2.80	Muscleblind-like 1 isoform 1D	1.66
Caveolin 2	-1.72	Muskelin intracellular mediator containing kelch motifs	1.30
CCR4 carbon catabolite repression 4-like	-2.18	Myosin heavy chain 9	3.12
Cell division cycle 5-like protein	1.63	Nascent polypeptide-associated complex subunit alpha	1.57
Cholinephosphotransferase 1	-1.71	NEDD8 precursor	-1.72
Chromatin-modifying protein 6	-1.30	Neural precursor cell developmentally down-regulated 4-like	1.65
Chromosome 1 open reading frame 156	2.74	N-myristoyltransferase 1a	-1.93
CI085 protein	2.12	Nucleolar and coiled-body phosphoprotein 1	1.80
Cirhin	2.61	Nucleolar GTP-binding protein 1	2.63
Coenzyme Q10 homolog B	-9.79	Nucleolar protein 5	2.11
Coiled-coil domain containing 47	-2.10	Nucleolar protein 5A	1.53
Cold shock domain-containing protein E1	1.90	Nucleoside diphosphate kinase 3	-3.11
Copper homeostasis protein cutC homolog	-1.86	PABPC4 protein	1.28
Cornichon homolog 4	-1.94	Peptidase D	1.51
Crystallin, zeta (quinone reductase)	1.41	Peptidyl-tRNA hydrolase domain containing 1	-1.94
CTP synthase	1.87	Phosducin-like protein 3	1.91
Cullin 2	-1.44	Phosphofurin acidic cluster sorting protein 2	1.88
Cyclin G2	-2.38	Plasminogen activator inhibitor type 1-like	-1.55
Cyclin-dependent kinase inhibitor 3	-3.18	Prefoldin subunit 6	-1.52
DCN1-like protein 1	1.49	Probable ATP-dependent RNA helicase DDX10	1.66
DCN1-like protein 5	-1.77	Probable ATP-dependent RNA helicase DDX41	1.44
DEAD (Asp-Glu-Ala-Asp) box polypeptide 39	-1.82	Probable ribosome biogenesis protein NEP1-like	1.91
Delta-9-desaturase 1	-6.26	Probable rRNA-processing protein EBP2	1.50
Der1-like domain member 1	-1.66	Profilin-2	-1.96
Dihydrofolate reductase	-1.79	Programmed cell death 5	-1.56
Dimethylglycine dehydrogenase	1.95	Proteasome (macropain) 26S, ATPase, 4	-2.16
DNA-directed RNA polymerase III subunit RPC5	1.85	Proteasome (macropain) 26S non-ATPase, 12	-1.70
EF-hand calcium-binding domain-containing protein 7	-3.67	Proteasome subunit alpha type-5	-2.06
Endothelial differentiation-related factor 1	-1.34	Proteasome subunit beta type-1-A	-1.60
Erythropoietin	1.81	Protein	-1.35
Eukaryotic translation initiation factor isoform 1B	-1.27	Protein DJ-1	-2.06
Eukaryotic translation initiation factor subunit D	1.26	Protein-L-isoaspartate (D-aspartate) O-methyltransferase	-1.92
Farnesyltransferase alpha subunit	-1.59	PRP6 pre-mRNA splicing factor 6 homolog	1.35
F-box protein 31	1.42	Purinergic receptor G-protein 5	3.80
F-box protein 9	-2.46	QIL1	-1.63
Fibropellin partial	2.08	Reticulon 1	-1.92
FK506-binding protein	-2.12	Ribosomal RNA processing protein 1 homolog B	1.90
Fragile X mental autosomal homolog 2	1.64	Ribosome biogenesis protein NSA2 homolog	1.65
General transcription factor IIH subunit 5	-1.59	RING-box protein 1	-1.43
Glycogenin 1	2.10		
Golgi reassembly stacking protein 1	-2.23		
Growth inhibition and differentiation related protein 86	1.54		

Gene Name	Fold-change	Gene Name	Fold-change
RIO kinase 1	1.93	Transmembrane emp24 domain-containing protein 9	-1.46
RNA polymerase-associated protein CTR9 homolog	1.34	Transmembrane protein 188	-1.58
RNA-binding protein PNO1	2.28	Trimeric intracellular cation channel type A	1.36
S-adenosylhomocysteine hydrolase	1.84	TTF1 protein	1.95
Selenophosphate synthetase 2	-1.80	Type I cytokeratin, enveloping layer	15.96
Serine/ threonine kinase 19	-4.75	Tyrosine 3-monooxygenase/tryptophan 5-monooxygenase activation epsilon polypeptide	-1.40
Serine/ threonine-protein kinase VRK3	-2.16		
Serpin H1	-2.38	Tyrosyl-tRNA synthetase	-2.37
Signal peptidase complex subunit 1	-1.47	U6 snRNA-associated Sm-like protein LSm5	-1.40
Small nuclear ribonucleoprotein E	-1.88	U6 snRNA-associated Sm-like protein LSm6	-1.76
Small VCP/ p97-interacting protein	1.83	Ubiquitin carboxyl-terminal hydrolase 14	-1.77
Splicing factor 3a subunit 1 isoform 2	1.30	Ubiquitin carboxyl-terminal hydrolase isozyme L3	-2.65
Surfeit 2	1.59	Ubiquitin domain-containing protein UFD1	-1.20
Surfeit 6	1.71	Ubiquitin-conjugating enzyme E2 A	-1.54
THAP domain-containing protein 2	1.73	Ubiquitin-conjugating enzyme E2 D2	-1.73
Thioredoxin domain-containing protein 17	-2.05	Ubiquitin-conjugating enzyme E2 L3	-1.77
Thioredoxin-like 1	-1.81	Ubiquitin-conjugating enzyme E2 variant 2	-1.52
Titin-like	1.32	Ubiquitin-conjugating enzyme E2A isoform 1	-1.55
TOB1 protein	2.24	Ubiquitin-conjugating enzyme E2N	-1.67
TRAF and TNF receptor-associated protein	-1.43	Uncharacterized protein C19orf12-like protein	-2.70
Transcription factor Dp-1	-1.35	UPF0466 protein mitochondrial-like	-1.80
Transcriptional repressor protein YY1	1.44	Voltage-dependent anion channel 2	1.66
Transducer of 1A	2.81	WD repeat-containing protein 75	2.19
Transducer of ERBB2	3.01	Zinc finger MYND domain-containing protein 17	1.69
Translational activator GCN1	1.97	Zinc transporter ZIP13	1.42
Translocon-associated protein subunit delta	-1.49		

Supplemental table A3.

Gene Name	Fold-change	Gene Name	Fold-change
5 -nucleotidase domain-containing protein 1	1.62	Mitochondrial ornithine transporter 1	-3.46
Acetyl-coenzyme A synthetase 2, mitochondrial-like	-1.59	Mitochondrial translation optimization 1 homolog, isoform 1	-1.82
Acyl-CoA desaturase	-5.53	Mitochondrial-processing peptidase subunit beta	-1.37
Acyl-CoA binding domain containing protein 7	-1.56	Mitoferrin-2	1.31
Adenosine kinase A	-1.59	Mitosis-specific chromosome segregation protein SMC1 homolog	1.42
Aldehyde dehydrogenase 7 family member A1	-1.85	Multidrug resistance associated protein 2	-1.53
Annexin A13	-1.97	NADH-cytochrome b5 reductase 2	-2.32
Annexin A2a	-2.93	Nattectin	-2.68
Anoctamin-8-like	1.67	Neural cell adhesion molecule isoform 3	1.84
Aspartate aminotransferase 1	1.51	Phosphoglucomutase 5	-1.38
ATP synthase lipid-binding protein mitochondrial	-1.51	Pitrilysin metalloproteinase	-2.10
ATP synthase mitochondrial F1 complex assembly factor 2	-1.65	Proliferating cell nuclear antigen	-1.85
ATP synthase F0 subunit 6	1.47	Prolylcarboxypeptidase (angiotensinase C)	-1.42
Beta-actin	-1.38	Propionyl-Co A carboxylase, alpha polypeptide	-1.96
Bromodomain adjacent to zinc finger domain protein 2B	1.28	Protein FAM101B-like	-1.49
Carboxymethylenebutenolidase homolog	-2.36	Protein FAM26E-like	-1.29
Cell death activator cide-3	-3.81	Rab interacting lysosomal protein 1	1.97
Coiled-coil-helix-coiled-coil-helix domain containing 3	-1.76	Ras GTPase-activating protein 1	1.81
Complement C1q tumor necrosis factor-related protein 5	-1.48	Ras-related C3 botulinum toxin substrate 1 (Rac1)	-1.71
CTD small phosphatase-like protein	1.46	Ras-related protein Rap-1b	-1.29
Cytochrome c oxidase subunit I	1.28	Repulsive guidance molecule-A	-1.33
Cytochrome c oxidase subunit mitochondrial	-2.54	Ring finger protein 220	1.52
Dehydrogenase/ reductase SDR family member 1	-3.43	Saccharopine dehydrogenase	-1.90
Dipeptidyl peptidase 3	-2.28	Selenoprotein H	-2.91
DnaJ homolog subfamily C member 11	-1.86	Septin 8a	-1.30
DnaJ homolog subfamily C member 17	-3.04	Serine/threonine-protein kinase SGK1	1.94
Fibronectin leucine rich transmembrane protein 3	-1.56	Short-chain dehydrogenase/reductase family protein	-1.91
FUN14 domain containing 1	-1.50	Skeletal muscle sodium channel alpha subunit-like	2.22
Gap junction alpha-1 protein	-1.52	SKI protein (class I)	1.29
Glucose-6-phosphate 1-dehydrogenase	-2.65	Solute carrier family member B3	7.41
Guanine nucleotide-binding protein GI/GS/GT subunit beta-1	-1.42	Sorting and assembly machinery component 50 homolog	-1.91
High mobility group protein B1	-1.32	Stem-loop binding protein	-2.24
Histone deacetylase 1B	-1.37	Telomerase protein component 1	-1.17
Hypoxanthine phosphoribosyltransferase 1 (Lesch-Nyhan syndrome)	1.46	Thioredoxin	-1.34
Isocitrate dehydrogenase 3 (NAD+) gamma	-1.78	Thymine-DNA glycosylase	-1.72
Isoform CRA_a	-1.52	Thymosin beta 4, X-linked	-1.17
Keratin 18	-1.56	Transcription elongation factor mitochondrial	4.84
Long-chain-fatty-acid-CoA- ligase ACSBG2	-5.10	Translocon-associated protein subunit alpha	1.72
LYR motif-containing protein 4	-1.48	Transmembrane protein C10orf57 homolog	-1.64
Mediator of RNA polymerase II transcription subunit 1	3.53	tRNA-nucleotidyltransferase 1, mitochondrial	-1.74
Membrane-type matrix metalloproteinase	-1.64	Tubulin beta-1	-1.59
Methylmalonic aciduria (cobalamin deficiency) cblD with homocystinuria	-1.62	Uncharacterized glycosyltransferase AER61-like	-1.52
Mitochondrial import receptor subunit TOM5 homolog	-1.47	Uncharacterized protein C7orf44-like isoform 1	-1.60
		Vav-3 protein	4.57
		WD repeat and FYVE domain-containing protein 1	5.33
		ZCCHC8 protein	-2.22
		Zinc finger E-box-binding homeobox 2 (Zeb2)	-1.35

Supplemental table A4.

Gene Name	Fold-change	Gene Name	Fold-change
3-mannosyl-glycoprotein 2-beta-N-acetylglucosaminyltransferase	-1.51	Chromobox protein homolog 5	-1.39
5 -AMP-activated protein kinase catalytic subunit alpha-1	1.55	Chromodomain helicase DNA binding protein 4	2.35
60S ribosomal protein L38	-1.71	Chromosome 5 open reading frame 24	-2.36
A230067G21Rik	2.12	Churchill domain containing 1	-1.30
Abnormal spindle-like microcephaly-associated protein homolog	1.61	CLASP1 protein	1.56
Actin-related protein 10	-1.34	Clathrin, light chain A	-1.32
Acyl-CoA synthetase long-chain family member 1	1.81	Coatomer subunit beta'- 2	-1.56
Adiponectin receptor protein 1	-1.76	Cohesin subunit Rad21	1.19
Alcohol dehydrogenase	-1.47	Coiled-coil domain-containing protein 75	-2.26
Alpha 3 (Goodpasture antigen) binding protein	2.31	COMM domain-containing protein 2	-1.34
Alpha tubulin	-2.26	Component of oligomeric golgi complex 7	-1.61
Alpha-1 globin	-8.66	Copper transport protein ATOX1	-1.63
Alpha-2 globin	-1.65	Coproporphyrinogen oxidase	-1.95
Alpha-2,6-sialyltransferase	2.22	Cornifelin homolog B	-1.99
Amyloid beta A4 protein	1.92	Creatine kinase, testis isozyme	-1.82
Androgen receptor	2.21	CREB/ATF bZIP transcription factor	1.51
Anion exchange protein 2	1.64	Cyclin L1	1.67
AP-4 complex subunit beta-1	1.84	Cyclin-dependent kinase 2	-2.43
Apoptosis-related protein 3	-1.80	Cyclin-dependent kinase 6	3.77
Aquaporin	1.61	Cyclin-dependent kinase 7	-1.23
Arrestin domain containing 1	1.83	Cysteine and histidine-rich domain-containing protein 1	1.47
Arrestin TRCarr	2.52	Cysteine-rich secretory protein LCCL domain-containing 2	4.05
Arsenate-resistance protein 2	1.43	Cytochrome b5	1.31
ASC protein	1.34	Cytochrome c oxidase subunit 7A	2.37
ATPase family AAA domain-containing protein 2	-2.23	Cytochrome c oxidase, subunit VIII	-1.91
ATPase, aminophospholipid transporter, class I, type 8B, member 1	2.34	Cytochrome P450 1A1	-1.95
AXIN1 Up-regulated 1	1.87	Cytochrome P450 3C1	1.28
Basic helix-loop-helix domain-containing protein KIAA2018	-1.26	Cytohesin-1	1.47
Basic leucine zipper transcriptional factor ATF-like	3.18	Danio rerio clone 1K20	1.61
Bloodthirsty	1.82	DDX5 protein	2.22
Bridging integrator 3	1.81	DEAD (Asp-Glu-Ala-Asp) box polypeptide 5	2.53
Bromodomain 4	1.56	Delangin isoform 3	1.28
Bromodomain-containing protein 4	1.25	Deoxyribose-phosphate aldolase-like	-1.31
BSG protein	-1.65	Diaphanous homolog 2	1.85
C18orf32 homolog	-1.29	Digestive cysteine proteinase 2	2.87
cAMP-dependent protein kinase catalytic subunit beta	-1.48	DNA mismatch repair protein	-1.82
Carbamoyl-phosphate synthetase 2, aspartate transcarbamylase, and dihydroorotase	-2.93	DNA polymerase delta catalytic subunit	-2.18
Carboxy-terminal domain, RNA polymerase II, polypeptide A	1.47	DNA replication complex GINS protein PSF2	-2.75
Caspase recruitment domain member 4 isoform 2	1.96	DNA-(cytosine5)-methyltransferase	-2.21
Caspase-3 precursor	-1.95	DNA-directed rRNA polymerase II subunit RPB7	-2.28
Catechol-O-methyltransferase domain-containing protein 1	-1.29	DnaJ (Hsp40) homolog, subfamily B, member 9	-2.13
Catenin (cadherin-associated protein), delta 1	2.22	Dnaj homolog subfamily B member 14	-1.17
Cathepsin C	-1.46	Dual-specificity tyrosine-(Y)-phosphorylation-regulated kinase 1A	1.49
Cathepsin L	-1.65	Dynamin 1-like	-1.92
CD151 antigen	-2.68	Dynamin 2	2.02
CDP-diacylglycerol--serine O-phosphatidyltransferase	2.74	EF-hand domain family, member A1	1.62
CEF-10	2.62	EF-hand domain-containing protein KIAA0494-like	1.42
Cellular retinoic acid-binding protein	-2.27	ELAV-like protein 1	1.76
Centaurin, beta 5, isoform CRA_b	2.48	Enhancer of polycomb homolog 1	1.47
Centromere protein m	-2.70	Ethanolamine kinase 1	2.53
Cerebral cavernous malformation 2	-1.61	Ethylmalonic encephalopathy 1	1.50
Chain C crystal structure of human G i1 bound to the GoLoco motif of RGS14	1.48	Ets variant gene 5 (ets-related molecule)	-1.65
Chibby homolog 1	-1.82	Eukaryotic translation initiation factor 4 gamma 2	1.85
CHK1 checkpoint homolog	-1.51	Exostosin-2	-1.46
Choline kinase beta	2.39	FAM49B protein	1.66
		Family with sequence similarity, member A	2.31
		Family with sequence similarity, member B	2.23
		Fatty acid synthase (Oleoyl-[acyl-carrier-protein] hydrolase)	-1.88
		Flotillin-1	-1.23
		Folliculin-interacting protein 1	4.27
		Forkhead-related transcription factor 1B, transcript variant 2	1.40

Gene Name	Fold-change	Gene Name	Fold-change
Four and a half LIM domains protein 2	-1.74	Lysosome-associated membrane glycoprotein 2	-1.60
Friend leukemia integration 1 transcription factor	1.86	Major facilitator superfamily domain-containing protein 5	-1.54
Fructose-bisphosphate aldolase C	-1.52	Mannose 6-phosphate receptor	-1.19
G protein-coupled receptor kinase interactor 2, isoform CRA_b	2.01	Mannose-P-dolichol utilization defect 1	-1.34
GA binding protein transcription factor, alpha subunit 60kda	-1.39	Mannoside acetylglucosaminyltransferase 2	1.75
Galactokinase 2	-1.71	Maturation-inducing protein	1.89
Galactosidase, beta 1-like	2.06	Member of RAS oncogene family-like 2A	2.93
Gamma-glutamyltransferase 5	2.24	Member RAS oncogene family	1.52
GC-rich sequence DNA-binding factor candidate isoform 1	1.66	Mesp	1.69
Gibelio Dazl	2.08	Mitochondrial cytochrome C oxidase subunit Vb	-1.60
GJ11255	2.41	Mitochondrial uncoupling protein 2	2.07
GL23181	1.51	Mitotin	-3.41
Glucosamine-6-phosphate deaminase 1	-1.62	MON2 protein	1.58
Glutathione peroxidase	-1.96	Myelin expression factor 2 (MYEF2)	2.63
Glutathione S-transferase	-2.18	Myogenic factor MYOD2	1.94
Glycosyltransferase 8 domain containing 1	-1.45	NAD+ poly (ADP-ribose) polymerase	-1.47
Granulito	-1.40	NADH dehydrogenase 1 alpha subcomplex subunit 11	1.99
Growth factor receptor-bound protein 14	2.16	Natural killer enhancing factor	-1.93
Guanine nucleotide binding protein (G protein) beta polypeptide 4	1.35	NECAP endocytosis associated 2	-1.20
Guanine nucleotide-binding protein G subunit alpha-2	2.13	NEDD8	-1.47
Heat shock protein 90kda, 1 beta isoform b	1.80	Neural precursor cell expressed, developmentally down-regulated 4	1.32
Hemoglobin subunit beta-1	-5.68	Nicotinamide phosphoribosyltransferase-like	1.88
HIRA interacting protein 3	-1.98	Notch homolog 2	1.95
Histidine triad nucleotide-binding protein 2	-1.25	Novel transposase	1.57
Histidine triad nucleotide-binding protein 3	-1.47	Nuclear prelamin A recognition factor	-2.10
Histone deacetylase 11	2.45	Nuclease HARBI1-like	1.68
HK domain containing, RNA binding, signal transduction associated 1	2.22	Nucleoredoxin-like protein 2	1.87
Homeodomain protein HOMEZ	1.78	Origin recognition complex, subunit 2	-1.49
Hox gene cluster	2.59	Ornithine decarboxylase antizyme 2	-1.24
HoxAb gene cluster	1.52	Osteocalcin	-1.35
Hyaluronidase-2	2.34	Perforin	1.53
Hyaluronoglucosaminidase 2	1.50	Phosphatase and actin regulator 1	1.77
Hypothetical protein TRIADDRAFT_58549	1.88	Phosphatidylinositol 4-kinase type 2-alpha	4.59
IL-6 subfamily member ciliary neurotrophic factor- like	-1.64	Phosphatidylinositol 4-kinase type II	-1.72
Immediate early response 3	1.70	Phosphatidylinositol binding clathrin assembly protein	1.54
Influenza virus NS1A-binding protein homolog A	1.66	Phosphatidylinositol N-acetylglucosaminyltransferase subunit H	-1.83
Inhibitor of growth family, member 5	-1.57	Phosphatidylinositol transfer protein beta isoform	1.80
Interleukin enhancer-binding factor 3 homolog	1.81	Phosphoglucose isomerase	-1.68
Intraflagellar transport protein 122 homolog	1.43	Phospholipase B domain containing 2	-1.50
Iodothyronine deiodinase type I	-1.43	Pituitary adenylate cyclase activating polypeptide receptor 1A	1.85
Isocitrate dehydrogenase	-1.91	Pituitary tumor-transforming gene 1 protein-interacting protein	1.48
Isthmin 1	3.04	PL10-related protein	1.93
KIAA0528 protein	2.30	PL-5283 protein	-1.52
Kinesin family member 13B	2.19	Pol-like protein	1.93
Latexin	-1.67	Poly (ADPribose) polymerase family, member 6, isoform CRA_e	2.32
Ldb1a protein	2.43	Poly A binding protein, cytoplasmic 1 b	1.84
Leucine rich repeat containing 45	2.41	Polymerase (DNA directed), delta 2, regulatory subunit 50kDa	-1.77
Leucine-rich repeats and calponin homology domain containing 4	1.73	Pre-mRNA-processing factor 39	2.09
Leucine-zipper-like transcription regulator 1	-1.50	Probable G-protein coupled receptor 125	1.53
LINE-1 reverse transcriptase homolog	1.54	Proline rich Gla (G-carboxyglutamic acid) 4	1.96
Lithognathus mormyrus clone lithmor1162	1.62	Proline-serine-threonine phosphatase-interacting protein 2	2.14
Liver carboxylesterase 2-like	3.66	Prosaposin	1.51
LON peptidase N-terminal domain and RING finger protein 1	1.80	Proteasome subunit, beta type-8	-1.89
Lysine-specific demethylase 5B	1.76	Protein Dok-7-like	-1.44
Lysine-specific demethylase 5B-like	2.04	Protein inhibitor of activated STAT, 3, isoform CRA_a	1.68
Lysine-specific demethylase 6B	1.27	Protein ITFG3	-1.54
Lysophosphatidic acid phosphatase type 6	-1.66		

Gene Name	Fold-change
Protein kinase, cAMP-dependent, regulatory, type II, alpha A	2.29
Protein LAP2 isoform 1	1.78
Protein NLRC3-like	1.91
Protein phosphatase 1 regulatory subunit 12C	-1.22
Protein tyrosine phosphatase, non-receptor type 2	2.12
Protein-glutamine gamma-glutamyltransferase 2	-2.03
Protein-kinase, interferon-inducible double stranded RNA dependent inhibitor, repressor of (p58 repressor)	-1.62
PRPF39 protein	1.49
Pumilio-like protein 1	1.77
Pyruvate dehydrogenase kinase, isoenzyme 2	23.60
Pyruvate dehydrogenase kinase, isozyme 3	1.62
Rab3 GTPase-activating protein non-catalytic subunit	2.00
Rad50-interacting protein 1	1.53
Ran-binding protein 3	1.70
Rapunzel 4	-1.60
Ras association domain-containing protein 1	1.63
Ras-related protein Rab-37	2.43
Regulator of chromosome condensation and BTB domain containing protein 1	1.49
Regulator of G-protein signaling 3	1.87
Renin receptor	-1.34
ReO_6	1.91
Replication factor C (activator 1) 37kDa	-1.95
Retinoblastoma binding protein 6	2.64
retinoic acid receptor alpha	1.91
Retinol dehydrogenase 14	2.29
Rho GTPase-activating protein 29	2.50
Riboflavin kinase	2.22
RNA binding motif protein 39	2.08
RNA-binding protein 40	2.40
RNase K b	-1.73
Sal-like 1a	1.64
Scaffold attachment factor B	1.49
Securin	-6.88
Sentrin-specific protease 2	1.34
Septin 2	-1.28
Serine carboxypeptidase 1	-1.39
Serine/threonine-protein kinase 16	1.43
Serine/threonine-protein phosphatase 2A, regulatory subunit B subunit alpha isoform 2	-1.49
Serpin peptidase inhibitor, clade A (alpha-1 antiproteinase, antitrypsin), member 10a	-1.51
SET translocation (myeloid leukemia-associated)	1.75
SH3 domain and tetratricopeptide repeats-containing protein 1	2.18
Signal peptidase complex subunit 3	-1.25
Signal-induced proliferation-associated 1	2.07
Sodium- and chloride-dependent taurine transporter	2.39
Sorbin and SH3 domain containing 2 isoform 8	1.62
Sorting nexin-5	-1.38
SOSS complex subunit C	-2.09
Spectrin repeat containig, nuclear envelope 1	2.40
Splicing factor 3a, subunit 3, 60kda	1.31
Splicing factor 3b subunit 1, 155kDa	1.59
Splicing regulatory glutamine/lysine-rich protein 1	2.01
Sterol carrier protein-2	2.01
Stromal interaction molecule 1	1.73
Structural maintenance of chromosomes protein 1A	1.79
Sulfiredoxin 1 homolog	-1.44
Suppressor of fused homolog	1.80
Synaptosomal-associated protein 23	1.43
Synaptosomal-associated protein 29	-1.42
Syndecan binding protein	-1.41
Syntaxin 4 isoform	1.63
Taeniopygia guttata similar to hCG2019360	4.97
Takifugu rubripes clone 214J14	1.79
Talin 1	1.91
TANK-binding kinase 1	-1.41
Targeting protein for Xklp2	-2.16
Taurine transporter	-1.49
Tax1 (human T-cell leukemia virus type I) binding protein 1B	2.24
Tc1-like transporase	1.71
Telomeric repeat binding factor (NIMA-interacting) 1	1.53
Telomeric repeat binding factor 2	1.33
Tetraspanin 5	-1.39
TGF-beta receptor type-2	1.59
Thioredoxin domain containing 4 (endoplasmic reticulum)	2.00
Thioredoxin reductase 1	-1.49
Thiosulfate sulfurtransferase KAT	-1.45
Thymidylate kinase	-2.07
Tight junction protein 1 isoform b	1.90
Titin-L1 fusion protein	1.83
T-lymphocyte 1 antigen-like protein	-2.57
TP53 apoptosis effector	1.65
TRAF-type zinc finger domain-containing protein 1	-1.55
Transcription factor CP2	2.67
Transcription factor SOX12	-2.46
Transient receptor potential cation channel subfamily M member 4	-1.59
Transmembrane 9 superfamily member 2	1.83
Transmembrane BAX inhibitor motif-containing protein 1	1.82
Transmembrane protein 134, isoform CRA_d	-1.53
Transposable element Tcb1 transposase	1.79
Transposase	3.22
Tripartite motif-containing 8	1.45
TRNA selenocysteine 1-associated protein 1-like	1.31
Tropomyosin alpha-4 chain	2.47
Truncated FBP32II and FBP32	2.20
Tubulin-folding cofactor B	1.70
Tumor necrosis factor receptor associated factor 2	2.43
Tyrosine-protein kinase JAK1	1.51
U1 small nuclear ribonucleoprotein 70 kDa	2.18
U2-associated protein SR140-like	1.61
Ubiquitin carboxyl-terminal hydrolase 22	2.04
Ubiquitin specific peptidase 33	1.42
Ubiquitin specific protease 48	1.61
Ubiquitin-conjugating enzyme E2 D4	1.57
Ubiquitin-conjugating enzyme UbcH5	2.30
Ubiquitin-like modifier-activating enzyme 1	1.66
UDP-Gal:betaGlcNAc beta 1,4-galactosyltransferase, polypeptide 4	1.52
UDP-N-acetylglucosamine-peptide N-acetylglucosaminyltransferase 110 kDa subunit	1.59
Uncharacterized protein C10orf18-like	2.26
UPF0462 protein C4orf33 homolog	-1.23
Vacuolar protein sorting-associating protein 4B	1.38
vacuolar-type H+ transporting ATPase B1 subunit	1.90
Venom dipeptidylpeptidase IV	-2.24
V-erb-a erythroblastic leukemia viral oncogene homolog 4	3.23
Very long-chain acyl-CoA-synthetase	2.43
Vesicle-associated membrane protein 3	1.94
Vesicle-associated membrane protein 5	-1.74
Voltage-dependent anion channel 1	-1.92
V-type proton atpase subunit E 1	-1.51
WD repeat domain 13	-1.53
WD repeat domain phosphoinositide-interacting protein 3	1.89
Wilms tumor 1 associated protein	1.34
XRCC5 protein	1.40

Gene Name	Fold-change	Gene Name	Fold-change
Zinc finger (C2H2 type) family protein	-1.34	Zinc finger protein 36, C3H type-like 1	1.35
Zinc finger BED domain-containing protein 4	2.19	Zinc finger protein 518A	1.42
Zinc finger CCCH domain-containing protein 7A	1.59	Zinc finger protein 572	2.00
Zinc finger protein	2.34	Zinc finger protein ubi-d4	1.26
Zinc finger protein 207	2.04	zinc finger protein, X-linked (ZFX)	2.24
Zinc finger protein 292	1.53		